Chapter 3
Stability and Convergence Analysis of ERKN Integrators for Second-Order ODEs with Highly Oscillatory Solutions

In this chapter, we commence the nonlinear stability and convergence analysis of ERKN integrators for second-order ODEs with highly oscillatory solutions, depending on a frequency matrix. As one of the most important applications, we also rigorously analyse the global errors of the blend of the ERKN time integrators and the Fourier pseudospectral spatial discretisation (ERKN-FP) when applied to semilinear wave equations. The theoretical results show that the nonlinear stability and the global error bounds are entirely independent of the frequency matrix, and the spatial mesh size. The analysis also provides a new perspective on the class of ERKN time integrators. That is, *the ERKN-FP methods are free from the restriction on the Courant-Friedrichs-Lewy (CFL) condition*.

3.1 Introduction

Nonlinear highly oscillatory problems occur in a variety of fields in science and engineering. The computation of nonlinear highly oscillatory problems contains numerous enduring challenges. In recent years, the investigation of efficient numerical methods for solving such problems has received increasing attention. In this chapter, we consider nonlinear multi-frequency highly oscillatory systems which can be formulated by the following initial value problem of second-order ODEs

$$\begin{cases} \ddot{q}(t) + \kappa^2 A q(t) = g\big(q(t)\big), \quad t \in [t_0, T], \\ q(t_0) = \varphi, \quad \dot{q}(t_0) = \psi, \end{cases} \tag{3.1}$$

where $\kappa^2 > 0$ is a takanami number, $q \in \mathbb{R}^d$, and $A \in \mathbb{R}^{d\times d}$ is a positive semi-definite matrix that implicitly contains the dominant frequencies of the highly oscillatory problem with $\kappa^2\|A\| \gg \max\left\{1, \left\|\frac{\partial g}{\partial q}\right\|\right\}$. This type of problem plays

X. Wu, B. Wang, *Geometric Integrators for Differential Equations with Highly Oscillatory Solutions*, https://doi.org/10.1007/978-981-16-0147-7_3

an important role in a wide variety of practical application areas in science and engineering, including nonlinear optics, molecular dynamics, solid state physics and quantum field theory. It is well known that the method of lines is an effective approach for the numerical integration of PDEs such as semilinear wave equations. With suitable spatial discretisation strategies, for example the finite difference method and the pseudospectral or spectral method (see, e.g. [1–6]), semilinear wave equations can be converted into highly oscillatory second-order ODEs (3.1). Therefore, research of the nonlinear multi-frequency highly oscillatory system (3.1) will also be significant for the numerical investigation of semilinear wave equations, including the important Klein–Gordon (KG) equation, in applications.

As is known, if the nonlinear function $g(\cdot)$ satisfies a Lipschitz condition, then the nonlinear highly oscillatory problem (3.1) has a unique solution (see, e.g. [7, 8]) over the interval $[t_0, T]$. Therefore, throughout this chapter we assume that the nonlinear function $g(\cdot)$ is locally Lipschitz continuous in a strip along the exact solution $q(t)$, i.e., there is a positive constant L, s.t.

$$\|g\big(\alpha(t)\big) - g\big(\beta(t)\big)\| \leqslant L\|\alpha(t) - \beta(t)\| \tag{3.2}$$

for all $t \in [t_0, T]$ and

$$\max\{\|\alpha(t) - q(t)\|,\ \|\beta(t) - q(t)\|\} \leqslant R. \tag{3.3}$$

The numerical treatment of the highly oscillatory system (3.1) has received a great deal of attention (see, e.g. [9–15]). Over the last decade, in order to systematically and comprehensively study the nonlinear multi-frequency highly oscillatory second-order ODEs (3.1) from both the analytical and numerical aspects, Wu et al. (see, e.g. [15, 16]) established the following matrix-variation-of-constants formula

$$\begin{cases} q(t) = \phi_0\big((t-t_0)^2\kappa^2 A\big)q(t_0) + (t-t_0)\phi_1\big((t-t_0)^2\kappa^2 A\big)\dot{q}(t_0) \\ \qquad\quad + \displaystyle\int_{t_0}^{t} (t-z)\phi_1\big((t-z)^2\kappa^2 A\big)g\big(q(z)\big)\mathrm{d}z, \\ \dot{q}(t) = -(t-t_0)\kappa^2 A\phi_1\big((t-t_0)^2\kappa^2 A\big)q(t_0) + \phi_0\big((t-t_0)^2\kappa^2 A\big)\dot{q}(t_0) \\ \qquad\quad + \displaystyle\int_{t_0}^{t} \phi_0\big((t-z)^2\kappa^2 A\big)g\big(q(z)\big)\mathrm{d}z, \end{cases} \tag{3.4}$$

where $t \in [t_0, T]$ and the functions $\phi_0(\mathbb{A})$ and $\phi_1(\mathbb{A})$ are defined by the following unconditionally convergent matrix-valued functions:

$$\phi_j(\mathbb{A}) := \sum_{k=0}^{\infty} \frac{(-1)^k \mathbb{A}^k}{(2k+j)!}, \quad j \in \mathbb{N}, \tag{3.5}$$

where $\mathbb{A}$ is a positive semi-definite matrix. Since the matrix A appearing in (3.4) is symmetric and positive semi-definite with $A = \Omega^2$, where Ω is also symmetric and

positive semi-definite, (3.4) can also read (see, e.g. [8, 10])

$$\begin{cases} q(t) = \cos((t-t_0)\kappa\Omega)q(t_0) + \kappa^{-1}\Omega^{-1}\sin\big((t-t_0)\kappa\Omega\big)\dot{q}(t_0) \\ \qquad + \int_{t_0}^{t} \kappa^{-1}\Omega^{-1}\sin((t-\tau)\kappa\Omega)g\big(q(\tau)\big)\mathrm{d}\tau, \\ \dot{q}(t) = -\kappa\Omega\sin((t-t_0)\kappa\Omega)q(t_0) + \cos((t-t_0)\kappa\Omega)\dot{q}(t_0) \\ \qquad + \int_{t_0}^{t} \cos((t-\tau)\kappa\Omega)g\big(q(\tau)\big)\mathrm{d}\tau. \end{cases} \tag{3.6}$$

It is noted that (3.6) depends on the decomposition of the matrix A, but (3.4) does not. Throughout this chapter we use (3.4).

The matrix-variation-of-constants formula (3.4) has received a lot of attention in the literature over the past decades. In particular, this formula can be used to design and analyse effective and efficient numerical integrators for solving the multi-frequency highly oscillatory system (3.1), such as the Gautschi-type methods of order two (see, e.g. [10, 11, 17, 18]), the exponentially fitted Runge–Kutta (EFRK) method [19], the exponentially fitted Runge–Kutta–Nyström (EFRKN) method [20], the functionally-fitted energy-preserving method [21], the adapted Runge–Kutta–Nyström (ARKN) method (see, e.g. [16, 22]), the extended Runge–Kutta–Nyström (ERKN) method (see, e.g. [23–27]), and arbitrarily high-order time-stepping methods (see, e.g. [28, 29]) and trigonometric Fourier collocation methods (see, e.g. [30, 31]). These methods share the fact that they can exactly integrate the unperturbed multi-frequency highly oscillatory system

$$q''(t) + \kappa^2 A q(t) = 0. \tag{3.7}$$

In particular, it is important to note that both the internal stages and updates of an ERKN integrator can solve (3.7) exactly. This property of ERKN method is essential for efficiently solving the nonlinear initial value problem (3.1) with highly oscillatory solutions. Therefore, ERKN integrators are oscillation preserving (see Chap. 1 for details and [32]).

Moreover, we also note that the classical stability analysis for numerical methods deals with the following prototype scalar test equation (see, e.g. [15, 33]):

$$\ddot{q}(t) + \omega^2 q(t) = -\varepsilon q(t) \quad \text{with} \quad \omega^2 + \varepsilon > 0, \tag{3.8}$$

where ω represents an estimate of the frequency λ and $\varepsilon = \lambda^2 - \omega^2$ is the error of the estimation. This is a linear system with a single-frequency, and hence this kind of stability analysis is termed as the linear stability analysis. However, it should be pointed out that the original system (3.1) is a nonlinear highly oscillatory system with multiple frequencies. In particular, it may be a large scale system of nonlinear multi-frequency highly oscillatory ODEs yielded by the refinement of spatial discretisations for semilinear wave equations. Therefore, it would be

insufficient to apply the linear and single frequency test equation (3.8) to the stability analysis for a numerical method designed for the nonlinear multi-frequency highly oscillatory system (3.1). This implies that it is important to investigate the nonlinear stability for (3.1). Taking into account the special structure brought by the linear term $\kappa^2 Aq(t)$ of the system, and approximating the nonlinear integrals appearing in the variation-of-constants formula (3.4) by suitable quadrature formulas, ERKN integrators for solving the nonlinear multi-frequency highly oscillatory system (3.1) have been proposed and developed in the literature. However, in contrast to classical methods, the theoretical analysis associated with ERKN integrators is not sufficient. Therefore, one of our main purposes in this chapter is to analyse the nonlinear stability and convergence for the ERKN integrators based on the matrix-variation-of-constants formula (3.4).

Another important issue in this chapter is to investigate the applications of ERKN time integrators to semilinear wave equations:

$$u_{tt}(x,t) - \varepsilon^2 \Delta u(x,t) + \rho u = f\big(u(x,t)\big), \quad x \in \mathbb{T} = \mathbb{R}/(2\pi\mathbb{Z}), \quad t \in [t_0, T], \tag{3.9}$$

where $\varepsilon^2 > 0$ and $\rho > 0$ are parameters, and the function $f(\cdot)$ is smooth and real-valued, satisfying $f(0) = 0$. The wave equation (3.9) is studied with 2π-periodic boundary conditions in one space dimension and its solution is assumed to be real-valued. The initial values at time $t = t_0$ are given by

$$u(x, t_0) = \varphi(x), \quad u_t(x, t_0) = \psi(x). \tag{3.10}$$

In the literature, there exist many numerical strategies for solving the semilinear wave equation, such as the finite difference method [3–5, 34], the pseudospectral or spectral method [2, 6], the radial basis functions methods [35], the dual reciprocity boundary integral equation technique [36] and the He's variational iteration method [37]. In this chapter, using the idea of the so-called operator-variation-of-constants formula described in Chap. 1, we will combine the ERKN time integrators with Fourier pseudospectral spatial discretisation (ERKN-FP) to solve (3.9) with 2π-periodic boundary conditions and initial conditions (3.10), and this leads to a fully discrete scheme. On the basis of energy techniques, which are widely used in the numerical analysis of partial differential equations (see, e.g. [38–44]), we will conclude that the global error bounds of the ERKN-FP schemes are independent of any restriction of the time stepsize and the spatial stepsize. Moreover, it is well known that restriction (CFL) of the time stepsize and the spatial stepsize for the traditional numerical schemes in the literature is required for solving semilinear wave equations. This means that the CFL condition is an essential element associated with numerical PDEs in practice and the traditional schemes for PDEs usually suffer from this crucial condition. Fortunately, however, our analysis of the global errors in this chapter confirms that the ERKN-FP schemes are completely independent of the CFL condition when applied to the semilinear

wave equation. This is one of the most essential properties of ERKN time integrators when applied to the semilinear wave equation.

3.2 Nonlinear Stability and Convergence Analysis for ERKN Integrators

This section concerns the study of nonlinear stability and convergence for ERKN integrators over a finite time interval. We begin this study with the nonlinear stability analysis of the matrix-variation-of-constants formula for the nonlinear highly oscillatory system (3.1), possessing multiple frequencies. After completing this, we turn to the nonlinear stability and convergence analysis for ERKN integrators. Throughout this section, $\|\cdot\|$ represents the vector 2-norm or matrix 2-norm (spectral norm).

3.2.1 Nonlinear Stability of the Matrix-Variation-of-Constants Formula

To begin with the stability analysis, we assume that the perturbed problem of (3.1) is

$$\begin{cases} \ddot{p}(t) + \kappa^2 A p(t) = g\big(p(t)\big) + \varepsilon(t), \quad t \in [t_0, T], \\ p(t_0) = \varphi + \tilde{\varphi}, \ \dot{p}(t_0) = \psi + \tilde{\psi}, \end{cases} \tag{3.11}$$

where A is symmetric and positive semi-definite, $\tilde{\varphi}$, $\tilde{\psi}$ are perturbations of the initial conditions, and $\varepsilon(t)$ is the perturbation of the nonlinear term. We let $\eta(t) = p(t) - q(t)$. Subtracting (3.1) from (3.11) leads to the following perturbation system:

$$\begin{cases} \ddot{\eta}(t) + \kappa^2 A \eta(t) = g\big(p(t)\big) - g\big(q(t)\big) + \varepsilon(t), \quad t \in [t_0, T], \\ \eta(t_0) = \tilde{\varphi}, \quad \dot{\eta}(t_0) = \tilde{\psi}. \end{cases} \tag{3.12}$$

We choose the time stepsize $\Delta t = (T - t_0)/N$, where N is a positive integer, and denote the steps as

$$t_n = t_0 + n\Delta t, \quad n = 0, 1, 2, \cdots, N.$$

Applying the matrix-variation-of-constants formula (3.4) to the perturbation system (3.12) yields

$$\begin{cases} \eta(t_n+\mu\Delta t) = \phi_0(\mu^2V)\eta(t_n) + \mu\Delta t\phi_1(\mu^2V)\dot{\eta}(t_n) \\ \qquad\qquad + \Delta t^2\int_0^\mu (\mu-z)\phi_1\big((\mu-z)^2V\big)\Big(g\big(p(t_n+z\Delta t)\big) - g\big(q(t_n+z\Delta t)\big)\Big)\mathrm{d}z \\ \qquad\qquad + \Delta t^2\int_0^\mu (\mu-z)\phi_1\big((\mu-z)^2V\big)\varepsilon(t_n+z\Delta t)\mathrm{d}z, \\ \dot{\eta}(t_n+\mu\Delta t) = -\mu\Delta t\kappa^2A\phi_1(\mu^2V)\eta(t_n) + \phi_0(\mu^2V)\dot{\eta}(t_n) \\ \qquad\qquad + \Delta t\int_0^\mu \phi_0\big((\mu-z)^2V\big)\Big(g\big(p(t_n+z\Delta t)\big) - g\big(q(t_n+z\Delta t)\big)\Big)\mathrm{d}z \\ \qquad\qquad + \Delta t\int_0^\mu \phi_0\big((\mu-z)^2V\big)\varepsilon(t_n+z\Delta t)\mathrm{d}z, \end{cases} \tag{3.13}$$

where $0 \leqslant \mu \leqslant 1$ and $V = \Delta t^2\kappa^2A$. Since the matrix A can be decomposed as $A = \Omega^2$, we denote the matrix $D = \kappa\Omega$, and then the decomposition of matrix κ^2A reads:

$$\kappa^2A = D^2,$$

where D is positive semi-definite matrix. Accordingly, the formula (3.13) can be rewritten as the following compact form:

$$\begin{aligned} \begin{bmatrix} D\eta(t_n+\mu\Delta t) \\ \dot{\eta}(t_n+\mu\Delta t) \end{bmatrix} &= \Psi(\mu,0,V)\begin{bmatrix} D\eta(t_n) \\ \dot{\eta}(t_n) \end{bmatrix} \\ &+\Delta t\int_0^\mu \Psi(\mu,z,V)\begin{bmatrix} 0 \\ g\big(p(t_n+z\Delta t)\big) - g\big(q(t_n+z\Delta t)\big) \end{bmatrix}\mathrm{d}z \\ &+\Delta t\int_0^\mu \Psi(\mu,z,V)\begin{bmatrix} 0 \\ \varepsilon(t_n+z\Delta t) \end{bmatrix}\mathrm{d}z, \end{aligned} \tag{3.14}$$

where

$$\Psi(\mu,z,V) = \begin{bmatrix} \phi_0((\mu-z)^2V) & \Delta t(\mu-z)D\phi_1((\mu-z)^2V) \\ -\Delta t(\mu-z)D\phi_1((\mu-z)^2V) & \phi_0((\mu-z)^2V) \end{bmatrix}. \tag{3.15}$$

Before going into the details of stability analysis, we summarise some useful properties related to the matrix-valued functions $\phi_j(\mu^2V)$ for $j \in \mathbb{N}$ and clarify the spectral norm of $\Psi(\mu,z,V)$ for $0 \leqslant \mu, z \leqslant 1$.

Lemma 3.1 (See, e.g. [28, 45]) *The matrix-valued functions defined by* (3.5) *satisfy*

$$\begin{aligned}&\int_0^1 (1-z)\phi_1\big(\mu^2(1-z)^2V\big)z^j\mathrm{d}z = \Gamma(j+1)\phi_{j+2}(\mu^2V), \quad j=0,1,2,\cdots,\\ &\int_0^1 \phi_0\big(\mu^2(1-z)^2V\big)z^j\mathrm{d}z = \Gamma(j+1)\phi_{j+1}(\mu^2V), \quad j=0,1,2,\cdots,\end{aligned} \tag{3.16}$$

where $\Gamma(j+1)$ *is the Gamma function.*

Lemma 3.2 *The matrix-valued functions defined by* (3.5) *are bounded, i.e.,*

$$\|\phi_j(\mu^2V)\| \leqslant \frac{1}{\Gamma(j+1)}, \quad j\in\mathbb{N}. \tag{3.17}$$

In particular, we have $\|\phi_0(\mu^2V)\| \leqslant 1$ *and* $\|\phi_1(\mu^2V)\| \leqslant 1$. *Moreover, we also have*

$$\|\mu\Delta t D\phi_1(\mu^2V)\| \leqslant 1 \quad \textit{and} \quad \|\mu\Delta t D\phi_j(\mu^2V)\| \leqslant \frac{1}{\Gamma(j)}, \quad j=2,3,\cdots, \tag{3.18}$$

where μ *is a positive number with* $0\leqslant\mu\leqslant 1$.

Proof The boundedness of $\|\phi_j(\mu^2V)\|$ and $\|\mu\Delta t D\phi_1(\mu^2V)\|$ can be confirmed straightforwardly from the definition of the matrix-valued functions (3.5) and Lemma 3.1. We thus need only to prove the boundedness of $\|\mu\Delta t D\phi_j(\mu^2V)\|$ for $j=2,3,\cdots$. Clearly, it follows from the definition of $\phi_j(\cdot)$ in (3.5) that

$$\mu\Delta t D(1-z)\phi_1\big(\mu^2(1-z)^2V\big) = \sin\big(\mu(1-z)\Delta t D\big).$$

Therefore, the conclusion of Lemma 3.1 yields that

$$\begin{aligned}\mu\Delta t D\phi_j(\mu^2V) &= \frac{\mu\Delta t D}{\Gamma(j-1)}\int_0^1 (1-z)\phi_1\big(\mu^2(1-z)^2V\big)z^{j-2}\mathrm{d}z\\ &= \frac{1}{\Gamma(j-1)}\int_0^1 \sin\big(\mu(1-z)\Delta t D\big)z^{j-2}\mathrm{d}z.\end{aligned} \tag{3.19}$$

Taking the spectral norms on both sides of (3.19) leads to

$$\|\mu\Delta t D\phi_j(\mu^2V)\| \leqslant \frac{1}{\Gamma(j-1)}\int_0^1 \|\sin\big(\mu(1-z)\Delta t D\big)\|z^{j-2}\mathrm{d}z \leqslant \frac{1}{\Gamma(j)}. \tag{3.20}$$

The statement of the lemma is confirmed. □

Lemma 3.3 (See, e.g. [13, 15]) *The bounded matrix-valued functions* $\phi_0(\mu^2 V)$ *and* $\phi_1(\mu^2 V)$ *defined by* (3.5) *satisfy*

$$\phi_0^2(\mu^2 V) + \mu^2 V \phi_1^2(\mu^2 V) = I, \tag{3.21}$$

where V *is any positive semi-definite matrix and* I *is the identity matrix.*

The other conclusions of Lemmas 3.1–3.3 can be proved by direct calculation, see [13, 15, 28, 45], and we here ignore the details of the proof.

Theorem 3.1 *The spectral norms of the matrices* $\Psi(\mu, z, V)$ *satisfy*

$$\|\Psi(\mu, z, V)\| = 1, \quad \forall\, \mu, z \in [0, 1], \tag{3.22}$$

where $V = h^2\kappa^2 A$ *and* A *is a symmetric and positive semi-definite matrix.*

Proof Obviously, the matrix $\Psi(\mu, z, V)$ is well defined in (3.15) because A is a symmetric and positive semi-definite matrix. Moreover, it is easy to verify that

$$\Psi(\mu, z, V)^{\intercal}\Psi(\mu, z, V) = I_{2d\times 2d}.$$

Thus, we have

$$\|\Psi(\mu, z, V)\| = 1, \quad \forall \mu, z \in [0, 1].$$

The conclusion of the lemma is confirmed. □

According to the assumption of the *finite-energy conditions* (see, e.g. [11, 12, 18])

$$\frac{1}{2}\|\dot{q}(t)\|^2 + \frac{\kappa^2}{2} q(t)^{\intercal} A q(t) \leqslant \frac{K^2}{2}, \tag{3.23}$$

where K is a constant, the error bounds of the Gaustchi-type methods of order two were proved to be independent of $\kappa^2\|A\|$. Here, we observe that Gautschi-type time integrators are special ERKN integrators of order two. Therefore, it seems reasonable to assume that the finite-energy condition (3.23) is also satisfied in a strip along the exact solution. Using this assumption, we will investigate the nonlinear stability and the error bounds of the ERKN integrators. To this end, we also need to quote the following Gronwall's inequality (see, e.g. [29]), which plays an important role for the remainder of our analysis.

Lemma 3.4 *Let* σ *be a positive number and* a_k, b_k $(k = 0, 1, 2, \cdots)$ *be nonnegative and satisfy*

$$a_k \leqslant (1 + \sigma\Delta t)a_{k-1} + \Delta t b_k, \quad k = 1, 2, 3, \cdots,$$

then

$$a_k \leqslant \exp(\sigma k\Delta t)\Big(a_0 + \Delta t \sum_{m=1}^{k} b_m\Big), \quad k = 1, 2, 3, \cdots.$$

In what follows, we first show the nonlinear stability of the matrix-variation-of-constants formula (3.4) whose perturbation formula is given by (3.13).

Theorem 3.2 *Assume that the solution $\eta(t)$ of the perturbation system (3.12) and its derivative $\dot{\eta}(t)$ satisfy the finite-energy condition. If the time stepsize Δt satisfies $\Delta t \leqslant \sqrt{\dfrac{1}{2L}}$, then we have*

$$\begin{aligned}
\|\eta(t_n)\| &\leqslant \exp\Big(T(1+4L)\Big)\Big(\|\tilde{\varphi}\| + \sqrt{\|\tilde{\psi}\|^2 + \kappa^2\tilde{\varphi}^{\intercal}A\tilde{\varphi}} + 4\Delta t\sum_{k=0}^{n}\max_{0\leqslant z\leqslant 1}\|\varepsilon(t_k+z\Delta t)\|\Big),\\
\|\dot{\eta}(t_n)\| &\leqslant \exp\Big(T(1+4L)\Big)\Big(\|\tilde{\varphi}\| + \sqrt{\|\tilde{\psi}\|^2 + \kappa^2\tilde{\varphi}^{\intercal}A\tilde{\varphi}} + 4\Delta t\sum_{k=0}^{n}\max_{0\leqslant z\leqslant 1}\|\varepsilon(t_k+z\Delta t)\|\Big).
\end{aligned} \tag{3.24}$$

That is, the matrix-variation-of-constants formula is nonlinearly stable over the time interval $[t_0, T]$.

Proof We take the l_2-norm on both sides of the first formula (3.13) and (3.14), respectively, and obtain

$$\begin{aligned}
\|\eta(t_n+\Delta t)\| \leqslant\ & \|\eta(t_n)\| + \Delta t\|\dot{\eta}(t_n)\| + \Delta t^2\int_0^1 \big\|g\big(p(t_n+z\Delta t)\big) - g\big(q(t_n+z\Delta t)\big)\big\|\mathrm{d}z\\
&+ \Delta t^2\int_0^1 \|\varepsilon(t_n+z\Delta t)\|\mathrm{d}z,
\end{aligned} \tag{3.25}$$

and

$$\begin{aligned}
&\sqrt{\|\dot{\eta}(t_n+\Delta t)\|^2 + \kappa^2\eta(t_n+\Delta t)^{\intercal}A\eta(t_n+\Delta t)} \leqslant \sqrt{\|\dot{\eta}(t_n)\|^2 + \kappa^2\eta(t_n)^{\intercal}A\eta(t_n)}\\
&+\Delta t\int_0^1 \big\|g\big(p(t_n+z\Delta t)\big) - g\big(q(t_n+z\Delta t)\big)\big\|\mathrm{d}z + \Delta t\int_0^1 \|\varepsilon(t_n+z\Delta t)\|\mathrm{d}z.
\end{aligned} \tag{3.26}$$

We then sum up the results in (3.25) and (3.26) and apply the Lipschitz condition. This leads to

$$\begin{aligned}
&\|\eta(t_n+\Delta t)\|+\sqrt{\|\dot\eta(t_n+\Delta t)\|^2+\kappa^2\eta(t_n+\Delta t)^{\intercal}A\eta(t_n+\Delta t)}\\
\leqslant\ &\|\eta(t_n)\|+\sqrt{\|\dot\eta(t_n)\|^2+\kappa^2\eta(t_n)^{\intercal}A\eta(t_n)}+\Delta t\|\dot\eta(t_n)\|+L\Delta t(1+\Delta t)\max_{0\leqslant z\leqslant 1}\|\eta(t_n+z\Delta t)\|\\
&+\Delta t(1+\Delta t)\max_{0\leqslant z\leqslant 1}\|\varepsilon(t_n+z\Delta t)\|.
\end{aligned}\tag{3.27}$$

It follows from the first equality in (3.13) that

$$\|\eta(t_n+\mu\Delta t)\|\leqslant\|\eta(t_n)\|+\Delta t\|\dot\eta(t_n)\|+\Delta t^2L\max_{0\leqslant z\leqslant 1}\|\eta(t_n+z\Delta t)\|+\Delta t^2\max_{0\leqslant z\leqslant 1}\|\varepsilon(t_n+z\Delta t)\|.$$

Under the assumption that time stepsize Δt satisfies $\Delta t\leqslant\sqrt{\dfrac{1}{2L}}$, we then obtain

$$\max_{0\leqslant z\leqslant 1}\|\eta(t_n+z\Delta t)\|\leqslant 2\|\eta(t_n)\|+2\Delta t\|\dot\eta(t_n)\|+2\Delta t^2\max_{0\leqslant z\leqslant 1}\|\varepsilon(t_n+z\Delta t)\|.\tag{3.28}$$

Inserting (3.28) into (3.27) gives

$$\begin{aligned}
&\|\eta(t_n+\Delta t)\|+\sqrt{\|\dot\eta(t_n+\Delta t)\|^2+\kappa^2\eta(t_n+\Delta t)^{\intercal}A\eta(t_n+\Delta t)}\\
\leqslant\ &\big(1+\Delta t(1+4L)\big)\Big(\|\eta(t_n)\|+\sqrt{\|\dot\eta(t_n)\|^2+\kappa^2\eta(t_n)^{\intercal}A\eta(t_n)}\Big)\\
&+2\Delta t(1+\Delta t)\max_{0\leqslant z\leqslant 1}\|\varepsilon(t_n+z\Delta t)\|.
\end{aligned}\tag{3.29}$$

Applying the Gronwall's inequality (Lemma 3.4) to (3.29) yields

$$\begin{aligned}
&\|\eta(t_n+\Delta t)\|+\sqrt{\|\dot\eta(t_n+\Delta t)\|^2+\kappa^2\eta(t_n+\Delta t)^{\intercal}A\eta(t_n+\Delta t)}\\
\leqslant\ &\exp\big(n\Delta t(1+4L)\big)\Big(\|\eta(t_0)\|+\sqrt{\|\dot\eta(t_0)\|^2+\kappa^2\eta(t_0)^{\intercal}A\eta(t_0)}\\
&+4\Delta t\sum_{k=0}^{n}\max_{0\leqslant z\leqslant 1}\|\varepsilon(t_k+z\Delta t)\|\Big).
\end{aligned}\tag{3.30}$$

We thus obtain the estimations

$$\|\eta(t_n)\| \leqslant \exp\Big(T(1+4L)\Big)\Big(\|\tilde{\varphi}\| + \sqrt{\|\tilde{\psi}\|^2 + \kappa^2\tilde{\varphi}^{\intercal}A\tilde{\varphi}} + 4\Delta t\sum_{k=0}^{n}\max_{0\leqslant z\leqslant 1}\|\varepsilon(t_k+z\Delta t)\|\Big),$$

$$\|\dot{\eta}(t_n)\| \leqslant \exp\Big(T(1+4L)\Big)\Big(\|\tilde{\varphi}\| + \sqrt{\|\tilde{\psi}\|^2 + \kappa^2\tilde{\varphi}^{\intercal}A\tilde{\varphi}} + 4\Delta t\sum_{k=0}^{n}\max_{0\leqslant z\leqslant 1}\|\varepsilon(t_k+z\Delta t)\|\Big).$$

Theorem 3.2 is proved. □

The matrix-variation-of-constants formula (3.4) is fundamental to a true understanding of ERKN integrators for the multi-frequency highly oscillatory system (3.1). Hence, its nonlinear stability is crucial for the nonlinear stability of ERKN integrators for (3.1).

3.2.2 *Nonlinear Stability and Convergence of ERKN Integrators*

The main theme of this subsection is the nonlinear stability and convergence analysis of ERKN integrators for the nonlinear multi-frequency highly oscillatory system (3.1). Choosing suitable nodes $c_1, c_2, \cdots, c_s$ and approximating the nonlinear integrals appearing in the formula (3.4) by suitable numerical quadrature formulae leads to the following ERKN integrators (see, e.g. [15]).

Definition 3.1 (See [15]) An s-stage multidimensional multi-frequency ERKN integrator with a stepsize Δt for the multidimensional and multi-frequency oscillatory nonlinear system (3.1) is defined as

$$\begin{cases} q_{n+1} = \phi_0(V)q_n + \Delta t\phi_1(V)\dot{q}_n + \Delta t^2\sum_{i=1}^{s}\bar{B}_i(V)g\big(Q_{ni}\big), \\ \dot{q}_{n+1} = -\Delta t\kappa^2 A\phi_1(V)q_n + \phi_0(V)\dot{q}_n + \Delta t\sum_{i=1}^{s}B_i(V)g\big(Q_{ni}\big), \\ Q_{ni} = \phi_0(c_i^2V)q_n + c_i\Delta t\phi_1(c_i^2V)\dot{q}_n + \Delta t^2\sum_{j=1}^{s}A_{ij}(V)g\big(Q_{nj}\big), \quad i = 1, 2, \cdots, s, \end{cases} \tag{3.31}$$

where $0 \leqslant c_i \leqslant 1$ for $i = 1, 2, \cdots, s$ are real constants and $\bar{B}_i(V)$, $B_i(V)$ and $A_{ij}(V)$ for $i, j = 1, 2, \cdots, s$ are matrix-valued functions of $V = \Delta t^2\kappa^2 A$.

Using the SSEN-tree set and the corresponding B-series theory (see, e.g. [13]), we now recall the order conditions of ERKN integrators which are summarised in the following theorem. The weights $\bar{B}_i(V)$, $B_i(V)$ and $A_{ij}(V)$ of an ERKN

integrator for $i, j = 1, 2, \cdots, s$ can be determined by the following order conditions.

Theorem 3.3 *The ERKN integrator (3.31) has order r if and only if the order conditions are satisfied*

$$\begin{aligned}
&\sum_{i=1}^{s} \bar{B}_i(V)\Phi_i(\tau) = \frac{\rho(\tau)!}{\tilde{\gamma}(\tau)s(\tau)}\phi_{\rho(\tau)+1}(V) + \mathscr{O}\big(\Delta t^{r-\rho(\tau)}\big), \quad \forall \tau \in \mathrm{SSRNT}_m, \quad m \leqslant r-1,\\
&\sum_{i=1}^{s} B_i(V)\Phi_i(\tau) = \frac{\rho(\tau)!}{\tilde{\gamma}(\tau)s(\tau)}\phi_{\rho(\tau)}(V) + \mathscr{O}\big(\Delta t^{r-\rho(\tau)+1}\big), \quad \forall \tau \in \mathrm{SSRNT}_m, \quad m \leqslant r,
\end{aligned} \tag{3.32}$$

where the definitions and properties of the order $\rho(\tau)$, the sgn $s(\tau)$, the density $\tilde{\gamma}(\tau)$, and the weight $\Phi_i(\tau)$ are well established and can be found in [13].

The conclusions of Theorem 3.3 indicate that the weights $\bar{B}_i(V)$, $B_i(V)$ and $A_{ij}(V)$ are the linear combination of $\phi_j(V)$. Furthermore, it is evident from the first conditions of (3.32) that the weights $\bar{B}_i(V)$ are independent of $\phi_0(V)$. Therefore, combining this fact with Lemma 3.2, we can establish the uniform boundedness of the weights $\bar{B}_i(V)$, $B_i(V)$ and $A_{ij}(V)$, which will be used in our theoretical analysis.

Lemma 3.5 *The weights $\bar{B}_i(V)$, $B_i(V)$ and $A_{ij}(V)$ are uniformly bounded, i.e.,*

$$\|\bar{B}_i(V)\| \leqslant \bar{B}, \quad \|\Delta t D\bar{B}_i(V)\| \leqslant \hat{B}, \quad \|B_i(V)\| \leqslant B, \quad \|A_{ij}(V)\| \leqslant \beta, \tag{3.33}$$

for $i, j = 1, 2, \cdots, s$, where $\bar{B}$, $\hat{B}$, B and β are all constants independent of Δt, κ^2 and the matrix V and D.

Applying an ERKN integrator (3.31) to the perturbed system (3.12), we obtain

$$\begin{cases}
\eta_{n+1} = \phi_0(V)\eta_n + \Delta t\phi_1(V)\dot{\eta}_n + \Delta t^2 \sum_{i=1}^{s} \bar{B}_i(V)\Big(g\big(P_{ni}\big) - g\big(Q_{ni}\big) + \varepsilon(t_n + c_i\Delta t)\Big),\\
\dot{\eta}_{n+1} = -\Delta t\kappa^2 A\phi_1(V)\eta_n + \phi_0(V)\dot{\eta}_n\\
\qquad\quad + \Delta t \sum_{i=1}^{s} B_i(V)\Big(g\big(P_{ni}\big) - g\big(Q_{ni}\big) + \varepsilon(t_n + c_i\Delta t)\Big),\\
\eta_{ni} = \phi_0(c_i^2V)\eta_n + c_i\Delta t\phi_1(c_i^2V)\dot{\eta}_n\\
\qquad\quad + \Delta t^2 \sum_{j=1}^{s} A_{ij}(V)\Big(g\big(P_{nj}\big) - g\big(Q_{nj}\big) + \varepsilon(t_n + c_j\Delta t)\Big),\\
i = 1, 2, \cdots, s.
\end{cases} \tag{3.34}$$

The first two equalities of (3.34) can be rewritten as the compact form:

$$\begin{bmatrix} D\eta_{n+1} \\ \dot{\eta}_{n+1} \end{bmatrix} = \Psi(1,0,V)\begin{bmatrix} D\eta_n \\ \dot{\eta}_n \end{bmatrix} + \Delta t \sum_{i=1}^{s} \begin{bmatrix} \Delta t D\bar{B}_i(V)\Big(g\big(P_{ni}\big) - g\big(Q_{ni}\big) + \varepsilon(t_n + c_i\Delta t)\Big) \\ B_i(V)\Big(g\big(P_{ni}\big) - g\big(Q_{ni}\big) + \varepsilon(t_n + c_i\Delta t)\Big) \end{bmatrix}. \tag{3.35}$$

We next present the nonlinear stability analysis for ERKN integrators over the finite time interval $[t_0, T]$.

Theorem 3.4 *It is assumed that the nonlinear function $g(\cdot)$ is locally Lipschitz continuous and the finite-energy condition (3.23) is satisfied. Then, if the time stepsize Δt satisfies the condition $\Delta t \leqslant \sqrt{\dfrac{1}{2sL\beta}}$, we have the following estimates for the perturbation system (3.12)*

$$\begin{aligned} \|\eta_n\| &\leqslant \exp(C_1 T)\left(\|\tilde{\varphi}\| + \sqrt{\|\tilde{\psi}\|^2 + \kappa^2\tilde{\varphi}^{\intercal}A\tilde{\varphi}} + C_2\Delta t\sum_{k=0}^{n}\sum_{i=1}^{s}\|\varepsilon(t_k + c_i\Delta t)\|\right), \\ \|\dot{\eta}_n\| &\leqslant \exp(C_1 T)\left(\|\tilde{\varphi}\| + \sqrt{\|\tilde{\psi}\|^2 + \kappa^2\tilde{\varphi}^{\intercal}A\tilde{\varphi}} + C_2\Delta t\sum_{k=0}^{n}\sum_{i=1}^{s}\|\varepsilon(t_k + c_i\Delta t)\|\right), \end{aligned} \tag{3.36}$$

where C_1 and C_2 are constants independent of Δt, κ^2 and the dominant frequency matrix A.

Proof Under the hypothesis of the finite-energy condition (3.23), by taking l^2-norm on both sides of the first equality in (3.34) and (3.35), we obtain

$$\|\eta_{n+1}\| \leqslant \|\eta_n\| + \Delta t\|\dot{\eta}_n\| + \Delta t^2\bar{B}\sum_{i=1}^{s}\Big(L\|\eta_{ni}\| + \|\varepsilon(t_n + c_i\Delta t)\|\Big),$$

and

$$\sqrt{\|\dot{\eta}_{n+1}\|^2 + \kappa^2\eta_{n+1}^{\intercal}A\eta_{n+1}} \leqslant \sqrt{\|\dot{\eta}_n\|^2 + \kappa^2\eta_n^{\intercal}A\eta_n} + \Delta t\big(\hat{B} + B\big)\sum_{i=1}^{s}\Big(L\|\eta_{ni}\| + \|\varepsilon(t_n + c_i\Delta t)\|\Big).$$

Summing up the above inequalities leads to

$$\|\eta_{n+1}\| + \sqrt{\|\dot{\eta}_{n+1}\|^2 + \kappa^2 \eta_{n+1}^{\mathsf{T}} A \eta_{n+1}} \leqslant \|\eta_n\| + \sqrt{\|\dot{\eta}_n\|^2 + \kappa^2 \eta_n^{\mathsf{T}} A \eta_n} + \Delta t \|\dot{\eta}_n\|$$
$$+\Delta t\big(\bar{B} + \hat{B} + B\big) \sum_{i=1}^{s} \Big(L\|\eta_{ni}\| + \|\varepsilon(t_n + c_i \Delta t)\| \Big), \tag{3.37}$$

where we have used the uniform boundedness of the weights $\bar{B}_i(V)$, $\Delta t D\bar{B}_i(V)$, $B_i(V)$, $A_{ij}(V)$ (see Lemma 3.5). Likewise, it follows from taking norms on both sides of the third equality in (3.34) that

$$\|\eta_{ni}\| \leqslant \|\eta_n\| + c_i \Delta t \|\dot{\eta}_n\| + \Delta t^2 \beta \sum_{i=1}^{s} \Big(L\|\eta_{ni}\| + \|\varepsilon(t_n + c_i \Delta t)\| \Big). \tag{3.38}$$

Under the assumption that the time stepsize Δt satisfies $\Delta t \leqslant \sqrt{\dfrac{1}{2sL\beta}}$, it then follows from the inequality (3.38) that

$$\sum_{i=1}^{s} \|\eta_{ni}\| \leqslant 2s\Big(\|\eta_n\| + \Delta t \|\dot{\eta}_n\| \Big) + \frac{1}{L} \sum_{i=1}^{s} \|\varepsilon(t_n + c_i \Delta t)\|. \tag{3.39}$$

Inserting (3.39) into (3.37) results in

$$\begin{aligned} &\|\eta_{n+1}\| + \sqrt{\|\dot{\eta}_{n+1}\|^2 + \kappa^2 \eta_{n+1}^{\mathsf{T}} A \eta_{n+1}} \\ \leqslant &\big(1 + C_1 \Delta t\big)\Big(\|\eta_n\| + \sqrt{\|\dot{\eta}_n\|^2 + \kappa^2 \eta_n^{\mathsf{T}} A \eta_n} \Big) \\ &+ C_2 \Delta t \sum_{i=1}^{s} \|\varepsilon(t_n + c_i \Delta t)\|, \end{aligned}$$

where $C_1 = 1 + sLC_2$ and $C_2 = 2\big(\bar{B} + \hat{B} + B\big)$ are constants. Thus, using the discrete Gronwall's inequality (Lemma 3.4), we obtain

$$\begin{aligned} &\|\eta_n\| + \sqrt{\|\dot{\eta}_n\|^2 + \kappa^2 \eta_n^{\mathsf{T}} A \eta_n} \\ \leqslant &\exp(C_1 T) \left(\|\tilde{\varphi}\| + \sqrt{\|\tilde{\psi}\|^2 + \kappa^2 \tilde{\varphi}^{\mathsf{T}} A \tilde{\varphi}} + C_2 \Delta t \sum_{k=0}^{n} \sum_{i=1}^{s} \|\varepsilon(t_k + c_i \Delta t)\| \right). \end{aligned}$$

This completes the proof. □

We denote

$$\zeta_n = q(t_n) - q_n, \quad \dot{\zeta}_n = \dot{q}(t_n) - \dot{q}_n, \quad \zeta_{ni} = q(t_n + c_i\Delta t) - Q_{ni} \quad \text{for} \quad i = 1, 2, \cdots, s.$$

Subtracting (3.31) from the exact solution (3.4) yields

$$\begin{cases} \zeta_{n+1} = \phi_0(V)\zeta_n + \Delta t\phi_1(V)\dot{\zeta}_n + \Delta t^2 \sum_{i=1}^{s} \bar{B}_i(V)\Big(g\big(q(t_n + c_i\Delta t)\big) - g(Q_{ni})\Big) \\ \qquad + \Delta t^2 \int_0^1 (1-z)\phi_1\big((1-z)^2 V\big) g\big(q(t_n + z\Delta t)\big)\mathrm{d}z - \Delta t^2 \sum_{i=1}^{s} \bar{B}_i(V) g\big(q(t_n + c_i\Delta t)\big), \\ \dot{\zeta}_{n+1} = -\Delta t\kappa^2 A\phi_1(V)\zeta_n + \phi_0(V)\dot{\zeta}_n + \Delta t \sum_{i=1}^{s} B_i(V)\Big(g\big(q(t_n + c_i\Delta t)\big) - g(Q_{ni})\Big) \\ \qquad + \Delta t \int_0^1 \phi_0\big((1-z)^2 V\big) g\big(q(t_n + z\Delta t)\big)\mathrm{d}z - \Delta t \sum_{i=1}^{s} B_i(V) g\big(q(t_n + c_i\Delta t)\big), \\ \zeta_{ni} = \phi_0(c_i^2 V)\zeta_n + c_i\Delta t\phi_1(c_i^2 V)\dot{\zeta}_n + \Delta t^2 \sum_{j=1}^{s} A_{ij}(V)\Big(g\big(q(t_n + c_j\Delta t)\big) - g(Q_{nj})\Big) \\ \qquad + c_i^2\Delta t^2 \int_0^1 (1-z)\phi_1\big((1-z)^2 c_i^2 V\big) g\big(q(t_n + zc_i\Delta t)\big)\mathrm{d}z \\ \qquad - \Delta t^2 \sum_{j=1}^{s} A_{ij}(V) g\big(q(t_n + c_j\Delta t)\big), \\ \qquad i = 1, 2, \cdots, s. \end{cases} \tag{3.40}$$

We then expand $g\big(q(t_n + z\Delta t)\big)$ at t_n into a Taylor series with remainder in integral form:

$$g\big(q(t_n + z\Delta t)\big) = \sum_{k=0}^{r-1} \frac{z^k \Delta t^k}{k!} g^{(k)}\big(q(t_n)\big) + \Delta t^r \int_0^z \frac{(z-\tau)^{r-1}}{(r-1)!} g^{(r)}\big(q(t_n + \tau\Delta t)\big)\mathrm{d}\tau. \tag{3.41}$$

Inserting the Taylor expression into the right-hand sides of (3.40) leads to

$$\begin{cases} \zeta_{n+1} = \phi_0(V)\zeta_n + \Delta t\phi_1(V)\dot{\zeta}_n + \Delta t^2 \sum_{i=1}^{s} \bar{B}_i(V)\Delta g_{ni} + \delta^{n+1}, \\ \dot{\zeta}_{n+1} = -\Delta t\kappa^2 A\phi_1(V)\zeta_n + \phi_0(V)\dot{\zeta}_n + \Delta t \sum_{i=1}^{s} B_i(V)\Delta g_{ni} + \dot{\delta}^{n+1}, \\ \zeta_{ni} = \phi_0(c_i^2 V)\zeta_n + c_i\Delta t\phi_1(c_i^2 V)\dot{\zeta}_n + \Delta t^2 \sum_{j=1}^{s} A_{ij}(V)\Delta g_{nj} + \Delta_{ni}, \quad i = 1, 2, \cdots, s, \end{cases} \tag{3.42}$$

where $\Delta g_{ni} = g\big(q(t_n + c_i\Delta t)\big) - g(Q_{ni})$ and the remainders can be explicitly represented as

$$\begin{aligned} \delta^{n+1} = & \sum_{k=0}^{r-1} \Delta t^{k+2} \left(\phi_{k+2}(V) - \sum_{i=1}^{s} \bar{B}_i(V)\frac{c_i^k}{k!} \right) g^{(k)}\big(q(t_n)\big) \\ & + \Delta t^{r+2} \int_0^1 (1-z)\phi_1\big((1-z)^2 V\big) \int_0^z \frac{(z-\tau)^{r-1}}{(r-1)!} g^{(r)}\big(q(t_n + \tau\Delta t)\big)\mathrm{d}\tau\mathrm{d}z \\ & - \Delta t^{r+2} \sum_{i=1}^{s} \bar{B}_i(V) \int_0^{c_i} \frac{(c_i-\tau)^{r-1}}{(r-1)!} g^{(r)}\big(q(t_n + \tau\Delta t)\big)\mathrm{d}\tau, \end{aligned} \tag{3.43}$$

$$\begin{aligned} \dot{\delta}^{n+1} = & \sum_{k=0}^{r-1} \Delta t^{k+1} \left(\phi_{k+1}(V) - \sum_{i=1}^{s} B_i(V)\frac{c_i^k}{k!} \right) g^{(k)}\big(q(t_n)\big) \\ & + \Delta t^{r+1} \int_0^1 \phi_0\big((1-z)^2 V\big) \int_0^z \frac{(z-\tau)^{r-1}}{(r-1)!} g^{(r)}\big(q(t_n + \tau\Delta t)\big)\mathrm{d}\tau\mathrm{d}z \\ & - \Delta t^{r+1} \sum_{i=1}^{s} B_i(V) \int_0^{c_i} \frac{(c_i-\tau)^{r-1}}{(r-1)!} g^{(r)}\big(q(t_n + \tau\Delta t)\big)\mathrm{d}\tau, \end{aligned} \tag{3.44}$$

and

$$\begin{aligned}\Delta_{ni} =& \sum_{k=0}^{r-1} \Delta t^{k+2} \left(c_i^{k+2} \phi_{k+2}(c_i^2 V) - \sum_{j=1}^{s} A_{ij}(V) \frac{c_j^k}{k!} \right) g^{(k)}\big(q(t_n)\big) \\ &+ c_i^{r+2} \Delta t^{r+2} \int_0^1 (1-z) \phi_1\big((1-z)^2 c_i^2 V\big) \int_0^z \frac{(z-\tau)^{r-1}}{(r-1)!} g^{(r)}\big(q(t_n + \tau c_i \Delta t)\big) \mathrm{d}\tau \mathrm{d}z \\ &- \Delta t^{r+2} \sum_{i=1}^{s} A_{i,j}(V) \int_0^{c_j} \frac{(c_j - \tau)^{r-1}}{(r-1)!} g^{(r)}\big(q(t_n + \tau \Delta t)\big) \mathrm{d}\tau. \end{aligned} \tag{3.45}$$

Note that if the weights $\bar{B}_i(V)$, $B_i(V)$ and $A_{ij}(V)$ satisfy the r-th order condition (3.32) in Lemma 3.3 and the exact solution of the multi-frequency highly oscillatory system (3.1) is of a suitable smoothness such that $g^{(r)} \in L^\infty\big([t_0, T], \mathbb{R}^d\big)$, then the remainders δ^{n+1}, $\dot{\delta}^{n+1}$ and Δ_{ni} satisfy the following estimates

$$\|\delta^{n+1}\| \leqslant \tilde{C}_1 \Delta t^{r+2}, \ \|\dot{\delta}^{n+1}\| \leqslant \tilde{C}_1 \Delta t^{r+1}, \ \sum_{i=1}^{s} \|\Delta_{ni}\| \leqslant \tilde{C}_1 \Delta t^{r+1}, \ \|D\delta^{n+1}\| \leqslant \tilde{C}_1 \Delta t^{r+1}, \tag{3.46}$$

where $\widetilde{C}_1$ is constant and obviously independent of Δt, the takanami number κ^2 and the dominant frequency-matrix A. Similarly to the stability analysis, we rewrite the first two equalities of (3.42) as the following matrix-vector form:

$$\begin{bmatrix} D\zeta_{n+1} \\ \dot{\zeta}_{n+1} \end{bmatrix} = \Psi(1, 0, V) \begin{bmatrix} D\zeta_n \\ \dot{\zeta}_n \end{bmatrix} + \Delta t \sum_{i=1}^{s} \begin{bmatrix} \Delta t D \bar{B}_i(V) \Delta g_{ni} \\ B_i(V) \Delta g_{ni} \end{bmatrix} + \begin{bmatrix} D\delta^{n+1} \\ \dot{\delta}^{n+1} \end{bmatrix}. \tag{3.47}$$

Taking norms on both sides of (3.47) and using the estimates in (3.46), we obtain

$$\sqrt{\|\dot{\zeta}_{n+1}\|^2 + \kappa^2 \zeta_{n+1}^{\mathsf{T}} A \zeta_{n+1}} \leqslant \sqrt{\|\dot{\zeta}_n\|^2 + \kappa^2 \zeta_n^{\mathsf{T}} A \zeta_n} + \Delta t L(\hat{B} + B) \sum_{i=1}^{s} \|\zeta_{ni}\| + \widetilde{C} \Delta t^{r+1}. \tag{3.48}$$

In what follows, we will investigate the convergence of the ERKN integrator (3.31) for solving the system (3.1) of nonlinear multi-frequency highly oscillatory second-order ODEs.

Theorem 3.5 *Assume that the weights $\bar{B}_i(V)$, $B_i(V)$ and $A_{ij}(V)$ satisfy the r-th order conditions (3.32) and the exact solution $q(t)$ of the nonlinear highly oscillatory system (3.1) satisfies suitable smoothness such that $g^{(r)} \in L^\infty\big([t_0, T], \mathbb{R}^d\big)$.*

Then, if the time stepsize Δt *satisfies* $\Delta t \leqslant \sqrt{\dfrac{1}{2sL\beta}}$, *we have the estimates*

$$\|q(t_n) - q_n\| \leqslant \widetilde{C}\Delta t^r \quad \text{and} \quad \|\dot{q}(t_n) - \dot{q}_n\| \leqslant \widetilde{C}\Delta t^r, \tag{3.49}$$

where the constant $\widetilde{C}$ *is independent of* Δt, κ^2 *and the dominant frequency-matrix* A.

Proof In a similar way to the proof of Theorem 3.4, it follows from taking norms on both sides of the first equation in (3.42) and summing up the obtained results with (3.48) that

$$\begin{aligned}\|\zeta_{n+1}\| + \sqrt{\|\dot{\zeta}_{n+1}\|^2 + \kappa^2 \zeta_{n+1}^{\mathsf{T}} A \zeta_{n+1}} \leqslant\ & \|\zeta_n\| + \sqrt{\|\dot{\zeta}_n\|^2 + \kappa^2 \zeta_n^{\mathsf{T}} A \zeta_n} + \Delta t \|\dot{\zeta}_n\| \\ & + \Delta t L(\bar{B} + \hat{B} + B) \sum_{i=1}^{s} \|\zeta_{ni}\| + 2\widetilde{C}_1 \Delta t^{r+1}.\end{aligned} \tag{3.50}$$

Taking norms on both sides of the third equation in (3.42) and noting that the time stepsize Δt satisfies $\Delta t \leqslant \sqrt{\dfrac{1}{2sL\beta}}$, we obtain

$$\sum_{i=1}^{s} \|\zeta_{ni}\| \leqslant 2s \left(\|\zeta_n\| + \Delta t \|\dot{\zeta}_n\| + \widetilde{C}_1 \Delta t^{r+1} \right). \tag{3.51}$$

Inserting (3.51) into (3.50) yields

$$\begin{aligned}& \|\zeta_{n+1}\| + \sqrt{\|\dot{\zeta}_{n+1}\|^2 + \kappa^2 \zeta_{n+1}^{\mathsf{T}} A \zeta_{n+1}} \\ \leqslant\ & \left(1 + C_1 \Delta t\right) \left(\|\zeta_n\| + \sqrt{\|\dot{\zeta}_n\|^2 + \kappa^2 \zeta_n^{\mathsf{T}} A \zeta_n} \right) + \left(sLC_2 \widetilde{C}_1 \Delta t + 2\widetilde{C}_1 \right) \Delta t^{r+1} \\ \leqslant\ & \left(1 + C_1 \Delta t\right) \left(\|\zeta_n\| + \sqrt{\|\dot{\zeta}_n\|^2 + \kappa^2 \zeta_n^{\mathsf{T}} A \zeta_n} \right) + \widetilde{C}_3 \Delta t^{r+1},\end{aligned}$$

where $\widetilde{C}_3 = sLC_2\widetilde{C}_1 + 2\widetilde{C}_1$ is a constant independent of Δt, κ^2 and $\|A\|$, whereas C_1 and C_2 are given in the proof of Theorem 3.4. Therefore, using the Gronwall's inequality (Lemma 3.4), we obtain

$$\begin{aligned}\|\zeta_n\| + \sqrt{\|\dot{\zeta}_n\|^2 + \kappa^2 \zeta_n^{\mathsf{T}} A \zeta_n} \leqslant\ & \exp\left(C_1 n \Delta t\right) \left(\|\zeta_0\| + \sqrt{\|\dot{\zeta}_0\|^2 + \kappa^2 \zeta_0^{\mathsf{T}} A \zeta_0} + \widetilde{C}_3 n \Delta t^{r+1} \right) \\ \leqslant\ & \widetilde{C}_3 T \exp\left(C_1 T\right) \Delta t^r \leqslant \widetilde{C} \Delta t^r,\end{aligned}$$

where $\widetilde{C} = \widetilde{C}_3 T \exp\left(C_1 T\right)$ is a constant independent of Δt, κ^2 and $\|A\|$. □

Theorem 3.5 shows an important fact that, with the finite-energy condition (3.23), the error bounds of an ERKN integrator for solving the system (3.1) of multi-frequency highly oscillatory second-order ODEs are independent of the takanami number κ^2, and the norm $\|A\|$ of the dominant frequency matrix A. This property is crucial for effectively and efficiently dealing with the system (3.1) of nonlinear multi-frequency highly oscillatory second-order ODEs.

Remark 3.2.1 According to the Theorem 3.4 and Theorem 3.5, the limitation of the time stepsize $\Delta t \leqslant \sqrt{\dfrac{1}{2sL\beta}}$ yields that the ERKN integrator for solving the system (3.1) is unconditionally stable and convergent.

3.3 ERKN Integrators with Fourier Pseudospectral Discretisation for Semilinear Wave Equations

This section presents an effective approach to the numerical solution of semilinear wave equation (3.9) by combining the ERKN time integrators with the Fourier pseudospectral spatial discretisation, which will have better computational efficiency than that of traditional schemes in the literature. The rigorous convergence analysis of the underlying numerical schemes will be based on energy techniques.

To simplify the analysis and practical computation, we truncate the whole space $\mathbb{R} = (-\infty, \infty)$ onto an interval $\Omega = (0, 2\pi)$ with periodic boundary conditions. We will only present and analyse the numerical schemes for the one-dimensional semilinear wave equation:

$$\begin{cases} u_{tt} - \varepsilon^2 \Delta u + \rho u = f(u), \quad (x,t) \in \Omega \times (t_0, T], \\ u(0,t) = u(2\pi,t), \quad u_t(0,t) = u_t(2\pi,t), \quad t \in [t_0, T], \\ u(x,t_0) = \varphi_1(x), \quad u_t(x,t_0) = \varphi_2(x), \quad x \in \bar{\Omega}, \end{cases} \tag{3.52}$$

where $\varepsilon^2 > 0$, $\rho > 0$ are parameters, and 2π is assumed to be the fundamental period. However, the generalisation to higher dimensions is straightforward and the result remains valid without modification.

3.3.1 Time Discretisation: ERKN Time Integrators

We here define $\mathscr{A}$ as the operator:

$$(\mathscr{A}v)(x) = (-\varepsilon^2 \Delta + \rho I)v(x),$$

where $\mathscr{A}$ is a linear, unbounded positive semi-definite operator, whose domain is

$$D(\mathscr{A}) := \left\{ v \in H^1(\Omega) : v(x) = v(x + 2\pi) \right\},$$

and $u(t)$ as the function that maps x to $u(t, x)$, i.e.

$$u(t) = [x \mapsto u(x, t)].$$

Then the semilinear wave equation can be formulated as the following abstract second-order ordinary differential equation:

$$\begin{cases} \ddot{u}(t) + \mathscr{A}u(t) = f\big(u(t)\big), \quad t_0 < t \leqslant T, \\ u(t_0) = \varphi_1(x), \quad \dot{u}(t_0) = \varphi_2(x), \end{cases} \tag{3.53}$$

where $\ddot{u}$ denotes the second-order temporal derivatives $\partial_t^2 u$. It follows from the *Duhamel Principle* that the solution of the abstract system (3.53) can be characterised by the following operator-variation-of-constants formula (see [28, 29, 45–49] for details).

Theorem 3.6 *The solution of the abstract ODE* (3.53) *and its derivative satisfy*

$$\begin{cases} u(t) = & \phi_0\big((t-t_0)^2\mathscr{A}\big)u(t_0) + (t-t_0)\phi_1\big((t-t_0)^2\mathscr{A}\big)\dot{u}(t_0) \\ & + \int_{t_0}^{t} (t-\zeta)\phi_1\big((t-\zeta)^2\mathscr{A}\big) f\big(u(\zeta)\big)\mathrm{d}\zeta, \\ \dot{u}(t) = & -(t-t_0)\mathscr{A}\phi_1\big((t-t_0)^2\mathscr{A}\big)u(t_0) + \phi_0\big((t-t_0)^2\mathscr{A}\big)\dot{u}(t_0) \\ & + \int_{t_0}^{t} \phi_0\big((t-\zeta)^2\mathscr{A}\big) f\big(u(\zeta)\big)\mathrm{d}\zeta, \end{cases}$$

for $t \geqslant t_0$, *where* $\phi_0\big((t-t_0)^2\mathscr{A}\big)$ *and* $\phi_1\big((t-t_0)^2\mathscr{A}\big)$ *are bounded operator-argument functions of* $\mathscr{A}$.

Clearly, the r-th order ERKN integrators (3.31) could be used for the temporal discretisation of the abstract ODE (3.53), i.e.,

$$\begin{cases} u^{n+1} = \phi_0(\mathscr{V})u^n + \Delta t\phi_1(\mathscr{V})\dot{u}^n + \Delta t^2 \sum_{i=1}^{s} \bar{B}_i(\mathscr{V}) f(u^{ni}), \\ \dot{u}^{n+1} = -\Delta t\mathscr{A}\phi_1(\mathscr{V})u^n + \phi_0(\mathscr{V})\dot{u}^n + \Delta t \sum_{i=1}^{s} B_i(\mathscr{V}) f(u^{ni}), \\ u^{ni} = \phi_0(c_i^2\mathscr{V})u^n + c_i\Delta t\phi_1(c_i^2\mathscr{V})\dot{u}^n + \Delta t^2 \sum_{j=1}^{s} A_{ij}(\mathscr{V}) f(u^{nj}), \quad i = 1, 2, \cdots, s, \end{cases} \tag{3.54}$$

where $\mathscr{V} = \Delta t^2 \mathscr{A}$ and $\phi_0(\mathscr{V})$, $\phi_1(\mathscr{V})$, $B_i(\mathscr{V})$, $\bar{B}_i(\mathscr{V})$ and $A_{ij}(\mathscr{V})$ are bounded operators.

3.3.2 Spatial Discretisation: Fourier Pseudospectral Method

We implement the spatial discretisation based on the Fourier pseudospectral method. To this end, we choose $\Delta x = 2\pi/M$ with the mesh size M, a positive even integer, to discrete the domain $\bar{\Omega}$. The grid points are denoted as $x_j = j\Delta x$ for $j = 0, 1, \cdots, M$. We define

$$X_M = \text{span}\left\{\mathrm{e}^{\mathrm{i}kx}, \quad k = -M/2, \cdots, M/2 - 1\right\}$$

and

$$Y_M = \left\{v = \big(v_0, v_1, \cdots, v_M\big)^{\mathsf{T}} \in \mathbb{R}^{M+1} \ : \ v_0 = v_M\right\}.$$

For a periodic function $v(x)$ defined on $\bar{\Omega}$ and a vector $v \in Y_M$, let $P_M : L^2(\bar{\Omega}) \to X_M$ be the standard L^2-projection operator, and $I_M : C(\bar{\Omega}) \to X_M$ or $Y_M \to X_M$ be the interpolation operator, i.e.

$$\big(P_M v\big)(x) = \sum_{k=-M/2}^{M/2-1} \hat{v}_k \mathrm{e}^{\mathrm{i}kx}, \qquad \big(I_M v\big)(x) = \sum_{k=-M/2}^{M/2-1} \tilde{v}_k \mathrm{e}^{\mathrm{i}kx}, \quad 0 \leqslant x \leqslant 2\pi,$$

where $\hat{v}_k$ and $\tilde{v}_k$ are the Fourier and discrete Fourier transform coefficients of the periodic function $v(x)$ and vector v, respectively, defined as

$$\hat{v}_k = \frac{1}{2\pi}\int_0^{2\pi} v(x)\mathrm{e}^{-\mathrm{i}kx}\mathrm{d}x \qquad \text{and} \qquad \tilde{v}_k = \frac{1}{M}\sum_{j=0}^{M-1} v_j \mathrm{e}^{-\mathrm{i}kx_j}.$$

To obtain the fully discrete scheme, the Fourier spectral method is used to discretise the ERKN integrators (3.54). This is described as follows. Find $u_M^{n+1}(x)$, $\dot{u}_M^{n+1}(x)$, $u_M^{ni}(x) \in X_M$, i.e.,

$$u_M^{n+1}(x) = \sum_{k=-M/2}^{M/2-1} \widehat{u}_k^{\,n+1} \mathrm{e}^{\mathrm{i}kx}, \quad \dot{u}_M^{n+1}(x) = \sum_{k=-M/2}^{M/2-1} \widehat{\dot{u}}_k^{\,n+1} \mathrm{e}^{\mathrm{i}kx}, \quad u_M^{ni}(x) = \sum_{k=-M/2}^{M/2-1} \widehat{u}_k^{\,ni} \mathrm{e}^{\mathrm{i}kx}, \tag{3.55}$$

such that

$$\begin{cases} \widehat{u}_k^{n+1} = \phi_0(\lambda_k^2)\widehat{u}_k^n + \Delta t\phi_1(\lambda_k^2)\widehat{\dot{u}}_k^n + \Delta t^2 \sum_{i=1}^{s} \bar{B}_i(\lambda_k^2) f\big(\widehat{u_M^{ni}(x)}\big)_k, \\ \widehat{\dot{u}}_k^{n+1} = -\Delta t\beta_k^2\phi_1(\lambda_k^2)\widehat{u}_k^n + \phi_0(\lambda_k^2)\widehat{\dot{u}}_k^n + \Delta t \sum_{i=1}^{s} B_i(\lambda_k^2) f\big(\widehat{u_M^{ni}(x)}\big)_k, \\ \widehat{u}_k^{ni} = \phi_0(c_i^2\lambda_k^2)\widehat{u}_k^n + c_i\Delta t\phi_1(c_i^2\lambda_k^2)\widehat{\dot{u}}_k^n + \Delta t^2 \sum_{j=1}^{s} A_{ij}(\lambda_k^2) f\big(\widehat{u_M^{nj}(x)}\big)_k, \\ \quad i = 1, 2, \cdots, s, \quad k = -M/2, \cdots, M/2-1, \end{cases} \tag{3.56}$$

where $\lambda_k^2 = \Delta t^2\beta_k^2$ with $\beta_k^2 = \rho + \varepsilon^2 k^2$ and $\phi_0(\lambda_k^2) = \cos(\lambda_k)$, $\phi_1(\lambda_k^2) = \dfrac{\sin(\lambda_k)}{\lambda_k}$. The blend of the ERKN time integrator and the Fourier spectral discretisation (ERKN-FS) can be represented by the Butcher tableau:

$$\begin{array}{c|c} c & A(\lambda_k^2) \\ \hline & \bar{B}^{\mathsf{T}}(\lambda_k^2) \\ \hline & B^{\mathsf{T}}(\lambda_k^2) \end{array} = \begin{array}{c|ccc} c_1 & A_{11}(\lambda_k^2) & A_{12}(\lambda_k^2) & \cdots & A_{1s}(\lambda_k^2) \\ c_2 & A_{21}(\lambda_k^2) & A_{22}(\lambda_k^2) & \cdots & A_{2s}(\lambda_k^2) \\ \vdots & \vdots & \vdots & & \vdots \\ c_s & A_{s1}(\lambda_k^2) & A_{s2}(\lambda_k^2) & \cdots & A_{ss}(\lambda_k^2) \\ \hline & \bar{B}_1(\lambda_k^2) & \bar{B}_2(\lambda_k^2) & \cdots & \bar{B}_s(\lambda_k^2) \\ \hline & B_1(\lambda_k^2) & B_2(\lambda_k^2) & \cdots & B_s(\lambda_k^2) \end{array}.$$

However, the computation of the Fourier coefficient defined in integral form is unsuitable in practice. In order to achieve an efficient implementation, we usually use the interpolation to replace the integral. Thus, the ERKN time integrator with the Fourier pseudospectral spatial discretisation (ERKN-FP) for the semilinear wave equation (3.52) can be formulated as follows.

Let

$$u_j^n \approx u(x_j, t_n), \quad \dot{u}_j^n \approx \partial_t u(x_j, t_n), \quad u_j^{ni} \approx u(x_j, t_n + c_i\Delta t), \quad j = 0, 1, \cdots, M,$$

and choose $u_j^0 = \varphi_1(x_j)$, $\dot{u}_j^0 = \varphi_2(x_j)$, we then have

$$u_j^{n+1} = \sum_{k=-M/2}^{M/2-1} \widetilde{u}_k^{n+1} \mathrm{e}^{\mathrm{i}kx_j}, \quad \dot{u}_j^{n+1} = \sum_{k=-M/2}^{M/2-1} \widetilde{\dot{u}}_k^{n+1} \mathrm{e}^{\mathrm{i}kx_j}, \quad u_j^{ni} = \sum_{k=-M/2}^{M/2-1} \widetilde{u}_k^{ni} \mathrm{e}^{\mathrm{i}kx_j}, \tag{3.57}$$

for $j = 0, 1, \cdots, M$, where

$$\begin{cases} \widetilde{u}_k^{n+1} = \phi_0(\lambda_k^2)\widetilde{u}_k^n + \Delta t\phi_1(\lambda_k^2)\widetilde{\dot{u}}_k^n + \Delta t^2 \sum_{i=1}^{s} \bar{B}_i(\lambda_k^2)\widetilde{f(u^{ni})}_k, \\ \widetilde{\dot{u}}_k^{n+1} = -\Delta t\beta_k^2\phi_1(\lambda_k^2)\widetilde{u}_k^n + \phi_0(\lambda_k^2)\widetilde{\dot{u}}_k^n + \Delta t \sum_{i=1}^{s} B_i(\lambda_k^2)\widetilde{f(u^{ni})}_k, \\ \widetilde{u}_k^{ni} = \phi_0(c_i^2\lambda_k^2)\widetilde{u}_k^n + c_i\Delta t\phi_1(c_i^2\lambda_k^2)\widetilde{\dot{u}}_k^n + \Delta t^2 \sum_{j=1}^{s} A_{ij}(\lambda_k^2)\widetilde{f(u^{nj})}_k, \\ \quad i = 1, 2, \cdots, s, \quad k = -M/2, \cdots, M/2 - 1. \end{cases} \tag{3.58}$$

It is obvious that the ERKN-FP method (3.57)–(3.58) can be efficiently implemented due to the fast Fourier transform (FFT). Its memory cost is $\mathscr{O}(M)$ and the computational cost per time step is $\mathscr{O}(M\log(M))$.

3.3.3 *Error Bounds of the ERKN-FP Method (3.57)–(3.58)*

Before dealing with the error estimation of the ERKN-FP method (3.57)–(3.58), we clarify some notations and assumptions:

- Denote the Soblev space

$$H_p^m(\Omega) = \left\{ u(x) \in H^m(\Omega) \;\middle|\; \partial_x^l u(0) = \partial_x^l u(2\pi),\ l = 0, 1, \cdots, m \right\}$$

  and the L^2-norm and the H^1-norm as:

$$\|v\|_{L^2}^2 = \sum_{k\in\mathbb{Z}} |\hat{v}_k|^2 \quad \text{and} \quad \|v\|_{H^1}^2 = \sum_{k\in\mathbb{Z}} (1+k^2)|\hat{v}_k|^2 \quad \text{with} \quad v(x) = \sum_{k\in\mathbb{Z}} \hat{v}_k \mathrm{e}^{\mathrm{i}kx}.$$

- The solutions $(u(x,t), \partial_t u(x,t))$ of the semilinear wave equation are studied in the space $H_p^1(\Omega) \times L^2(\Omega)$ with the energy norm:

$$|||(u, \partial_t u)||| = \sqrt{\|u\|_{H^1}^2 + \|\partial_t u\|_{L^2}^2}.$$

- Assume that the nonlinear function $f(\cdot)$ and the exact solution of the semilinear wave equation (3.52) satisfy

$$f(\cdot) \in C^r(\mathbb{R}), \quad u \in C^r\left([0,T], H_p^{m_0+1}(\Omega)\right) \quad (m_0 \geqslant 1, r \geqslant 0).$$

Under this assumption, we denote

$$K_1 = \max\left\{\|u(\cdot,t)\|_{L^\infty([0,T];H^1)},\ \|\partial_t u(\cdot,t)\|_{L^\infty([0,T];L^2)}\right\} \lesssim 1$$

and

$$K_2 = \max_{0\leqslant l\leqslant r}\ \max_{\|w\|_{L^2}\leqslant K_1} \left\|f^{(l)}(w)\right\|_{L^2} \lesssim 1.$$

With $u_k^n, \dot{u}_k^n$ and u_k^{ni}, which are obtained from (3.57)–(3.58), define the error functions as

$$\begin{aligned} e^n(x) :=& u(x,t_n) - \left(I_M u^n\right)(x),\\ \dot{e}^n(x) :=& u(x,t_n) - \left(I_M \dot{u}^n\right)(x),\\ e^{ni}(x) :=& u(x,t_n+c_i\Delta t) - \left(I_M u^{ni}\right)(x). \end{aligned}$$

To proceed to the proof of the error bound for the ERKN-FP method, we define the projected error as

$$\begin{aligned} e_M^n(x) :=& P_M u(x,t_n) - u_M^n(x),\\ \dot{e}_M^n(x) :=& P_M \partial_t u(x,t_n) - \dot{u}_M^n(x),\\ e_M^{ni}(x) :=& P_M u(x,t_n+c_i\Delta t) - u_M^{ni}(x), \end{aligned}$$

where $u_M^n(x)$, $\dot{u}_M^n(x)$ and $u_M^{ni}(x)$ are yielded from the ERKN-FS method (3.55)–(3.56). It then follows from the triangle inequality and estimates on the projection error [6, 50] that

$$\begin{aligned} \|e^n\|_{H^1} + \|\dot{e}^n\|_{L^2} \leqslant\ & \|e_M^n\|_{H^1} + \|\dot{e}_M^n\|_{L^2} + \|u_M^n(\cdot) - \left(I_M u^n\right)(\cdot)\|_{H^1} + \|\dot{u}_M^n(\cdot) - \left(I_M \dot{u}^n\right)(\cdot)\|_{L^2}\\ &+ \|u(\cdot,t_n) - P_M u(\cdot,t_n)\|_{H^1} + \|\partial_t u(\cdot,t_n) - P_M\partial_t u(\cdot,t_n)\|_{L^2}\\ \lesssim\ & \|e_M^n\|_{H^1} + \|\dot{e}_M^n\|_{L^2} + \Delta x^{m_0}, \end{aligned} \tag{3.59}$$

and

$$\begin{aligned} \|e^{ni}\|_{L^2} \leqslant\ & \|e_M^{ni}\|_{L^2} + \|u_M^{ni}(\cdot) - \left(I_M u^{ni}\right)(\cdot)\|_{L^2} + \|u(\cdot,t_{ni}) - P_M u(\cdot,t_{ni})\|_{L^2}\\ \lesssim\ & \|e_M^n\|_{L^2} + \Delta x^{m_0+1}. \end{aligned}$$

Hence, the error estimates for the ERKN-FP methods can be converted to the estimates for the ERKN-FS methods. Moreover, the theoretical analysis for PDEs is quite different from that for ODEs. In particular, the assumption for the nonlinear function $f(\cdot)$ satisfying the Lipschitz condition will not be the same. Fortunately, the

boundedness of the numerical solutions will be helpful to the theoretical analysis. In what follows, we will first analyse the boundedness of the numerical solutions for the ERKN-FS methods (3.55)–(3.56). We then will deduce the convergence of the ERKN-FP methods (3.57)–(3.58).

With regard to the boundedness of the numerical methods, we start with the explicit ERKN-FS methods (3.55)–(3.56), which can be expressed as

$$\begin{cases} \widehat{u}_k^{n+1} = \phi_0(\lambda_k^2)\widehat{u}_k^n + \Delta t\phi_1(\lambda_k^2)\widehat{\dot{u}}_k^n + \Delta t^2 \sum_{i=1}^{s} \bar{B}_i(\lambda_k^2) f\big(\widehat{u_M^{ni}(x)}\big)_k, \\ \widehat{\dot{u}}_k^{n+1} = -\Delta t\beta_k^2\phi_1(\lambda_k^2)\widehat{u}_k^n + \phi_0(\lambda_k^2)\widehat{\dot{u}}_k^n + \Delta t \sum_{i=1}^{s} B_i(\lambda_k^2) f\big(\widehat{u_M^{ni}(x)}\big)_k, \\ \widehat{u}_k^{ni} = \phi_0(c_i^2\lambda_k^2)\widehat{u}_k^n + c_i\Delta t\phi_1(c_i^2\lambda_k^2)\widehat{\dot{u}}_k^n + \Delta t^2 \sum_{j=1}^{i-1} A_{ij}(\lambda_k^2) f\big(\widehat{u_M^{nj}(x)}\big)_k, \\ \quad i = 1, 2, \cdots, s, \quad k = -M/2, \cdots, M/2-1, \end{cases} \tag{3.60}$$

with the Butcher tableau:

$$\begin{array}{c|c} c & A(\lambda_k^2) \\ \hline & \bar{B}^{\mathsf{T}}(\lambda_k^2) \\ \hline & B^{\mathsf{T}}(\lambda_k^2) \end{array} = \begin{array}{c|cccc} c_1 & 0 & 0 & \cdots & 0 & 0 \\ c_2 & A_{21}(\lambda_k^2) & 0 & \cdots & 0 & 0 \\ \vdots & \vdots & \vdots & & \vdots & \vdots \\ c_s & A_{s1}(\lambda_k^2) & A_{s2}(\lambda_k^2) & \cdots & A_{s,s-1}(\lambda_k^2) & 0 \\ \hline & \bar{B}_1(\lambda_k^2) & \bar{B}_2(\lambda_k^2) & \cdots & \bar{B}_{s-1}(\lambda_k^2) & \bar{B}_s(\lambda_k^2) \\ \hline & B_1(\lambda_k^2) & B_2(\lambda_k^2) & \cdots & B_{s-1}(\lambda_k^2) & B_s(\lambda_k^2) \end{array}.$$

Theorem 3.7 (Boundedness for a Single Time Step: Explicit ERKN-FS Method) *Let the weights $\bar{B}_i(\lambda_k^2)$, $B_i(\lambda_k^2)$ and $A_{ij}(\lambda_k^2)$ of the explicit ERKN-FS method (3.55)–(3.60) satisfy the r-th order conditions (3.32). There exists a sufficiently small $0 < \tau_0 \leqslant 1$ such that the time stepsize $\Delta t \leqslant \tau_0$. If the numerical solution $(u_M^n, \dot{u}_M^n) \in H_p^1(\Omega) \times L^2(\Omega)$ of the explicit ERKN-FS method satisfies $|||(u_M^n, \dot{u}_M^n)||| \leqslant K$, then we have*

$$\|u_M^{ni}\| \lesssim 1, \quad i = 1, 2, \cdots, s,$$

and $(u_M^{n+1}, \dot{u}_M^{n+1}) \in H_p^1(\Omega) \times L^2(\Omega)$ with

$$\|u_M^{n+1}\|_{H^1} \leqslant C_K \quad \text{and} \quad \|\dot{u}_M^{n+1}\|_{L^2} \leqslant C_K,$$

where C_K is independent of the time stepsize Δt and spatial mesh size M.

Proof 1. *"Estimations for update stage procedures: $u_M^{n+1}(x)$ and $\dot{u}_M^{n+1}(x)$".*
For the first equality in (3.60), an application of the triangle inequality results in

$$|\widehat{u}_k^{n+1}| \leqslant |\widehat{u}_k^n| + \Delta t|\widehat{\dot{u}}_k^n| + \Delta t^2 \bar{B} \sum_{i=1}^{s} |\widehat{f\left(u_M^{ni}(x)\right)}_k|$$

and

$$\sqrt{1+k^2}\left|\widehat{u}_k^{n+1}\right| \leqslant \sqrt{1+k^2}\left|\widehat{u}_k^n\right| + \frac{\sqrt{1+k^2}}{\sqrt{\rho+\varepsilon^2 k^2}}\left|\widehat{\dot{u}}_k^n\right| + \Delta t \hat{B} \sum_{i=1}^{s} \left|\widehat{f(u^{nj})}_k\right|.$$

Then, applying Minkowski's inequality and Parseval's identity to the above inequalities, we have

$$\|u_M^{n+1}\|_{L^2} \leqslant \|u_M^n\|_{L^2} + \Delta t\|\dot{u}_M^n\|_{L^2} + \Delta t^2 \bar{B} \sum_{i=1}^{s} \left\| P_M f\left(u_M^{ni}\right)\right\|_{L^2} \tag{3.61}$$

and

$$\|u_M^{n+1}\|_{H^1} \leqslant \|u_M^n\|_{H^1} + \varsigma\|\dot{u}_M^n\|_{L^2} + \Delta t \hat{B} \sum_{i=1}^{s} \left\| P_M f\left(u_M^{ni}\right)\right\|_{L^2}, \tag{3.62}$$

where $\varsigma = 1/\min\left\{\sqrt{\rho}, \varepsilon\right\} > 0$ is a constant parameter. Likewise, it follows from the second equality in (3.60) that

$$\begin{aligned} |\widehat{\dot{u}}_k^{n+1}| &\leqslant \sqrt{\rho+\varepsilon^2 k^2}|\widehat{u}_k^n| + |\widehat{\dot{u}}_k^n| + \Delta t B \sum_{i=1}^{s} |\widehat{f\left(u_M^{ni}(x)\right)}_k| \\ &\leqslant \varrho\sqrt{1+k^2}|\widehat{u}_k^n| + |\widehat{\dot{u}}_k^n| + \Delta t B \sum_{i=1}^{s} |\widehat{f\left(u_M^{ni}(x)\right)}_k|, \end{aligned}$$

where $\varrho = \max\{\sqrt{\rho}, \varepsilon\} > 0$ is also a constant parameter. Similarly, we have the following estimate

$$\|\dot{u}_M^{n+1}\|_{L^2} \leqslant \varrho\|u_M^n\|_{H^1} + \|\dot{u}_M^n\|_{L^2} + \Delta t B \sum_{i=1}^{s} \left\| P_M f\left(u_M^{ni}\right)\right\|_{L^2}. \tag{3.63}$$

Consequently, summing up (3.62) and (3.63) leads to

$$\|u_M^{n+1}\|_{H^1} + \|\dot{u}_M^{n+1}\|_{L^2} \leqslant \hat{C}_1\Big(\|u_M^n\|_{H^1} + \|\dot{u}_M^n\|_{L^2}\Big) + \Delta t\big(\hat{B} + B\big)\sum_{i=1}^{s}\Big\|f\big(u_M^{ni}\big)\Big\|_{L^2}, \tag{3.64}$$

where $\hat{C}_1 = \max\big\{\varrho, \varsigma\big\} + 1$ is a constant parameter.

2. *"Estimations for internal stage procedures: $u_M^{ni}(x)$".*
Using the third equality in (3.60), we obtain

$$\big|\widehat{u}_k^{ni}\big| \leqslant \big|\widehat{u}_k^{n}\big| + c_i\Delta t\big|\widehat{\dot{u}}_k^{n}\big| + \Delta t^2\beta\sum_{j=1}^{i-1}\big|\widehat{f(u^{nj})}_k\big|.$$

Applying Minkowski's inequality and Parseval's identity to the above inequality yields

$$\|u_M^{n1}\|_{L^2} \leqslant \|u_M^n\|_{L^2} + c_i\Delta t\|\dot{u}_M^n\|_{L^2},$$

$$\|u_M^{ni}\|_{L^2} \leqslant \|u_M^n\|_{L^2} + c_i\Delta t\|\dot{u}_M^n\|_{L^2} + \Delta t^2\beta\sum_{j=1}^{i-1}\big\|P_M f(u_M^{nj})\big\|_{L^2}, \quad i = 2, \cdots, s. \tag{3.65}$$

3. *"Boundedness of the numerical solutions".*
According to the inequalities of (3.65), if the solution $(u_M^n, \dot{u}_M^n) \in H_p^1(\Omega) \times L^2(\Omega)$ of the explicit ERKN-FS method (3.55)–(3.60) satisfies

$$|||(u_M^n, \dot{u}_M^n)||| \leqslant K,$$

then, the following approximations can be obtained by recursion:

$$\|u_M^{ni}\|_{L^2} \leqslant (1 + \Delta t)^i K \lesssim 1, \qquad i = 1, 2, \cdots, s, \tag{3.66}$$

where we have used the fact that $\|u_M^n\|_{L^2} \leqslant \|u_M^n\|_{H^1} \leqslant K$ and the sufficiently small time stepsize Δt such that $\Delta t\beta K_2 \leqslant 1$. Inserting the result (3.66) into (3.64)

yields

$$\begin{aligned}\|u_M^{n+1}\|_{H^1}+\|\dot{u}_M^{n+1}\|_{L^2} \leqslant\ & \hat{C}_1\Big(\|u_M^n\|_{H^1}+\|\dot{u}_M^n\|_{L^2}\Big)\\ &+\Delta t\big(\hat{B}+B\big)\sum_{i=1}^{s}\Big\|\int_0^1 f'\big(\tau u_M^{ni}\big)\mathrm{d}\tau\cdot u_M^{ni}\Big\|_{L^2}\\ \leqslant\ & \hat{C}_1\Big(\|u_M^n\|_{H^1}+\|\dot{u}_M^n\|_{L^2}\Big)+\Delta t\big(\hat{B}+B\big)K_2\sum_{i=1}^{s}\|u_M^{ni}\|_{L^2}\\ \leqslant\ & \hat{C}_2\Big(1+\Delta t+\Delta t\sum_{i=1}^{s}(1+\Delta t)^i\Big)\leqslant C_K,\end{aligned}$$

where $\hat{C}_2=K_1\max\Big\{\hat{C}_1,(\hat{B}+B)K_2\Big\}$ is a constant and C_K is obviously independent of time stepsize Δt and spatial mesh size M. □

For the implicit ERKN-FS method (3.55)–(3.56):

$$\begin{cases}\widehat{u}_k^{\,n+1}=\phi_0(\lambda_k^2)\widehat{u}_k^{\,n}+\Delta t\phi_1(\lambda_k^2)\widehat{\dot{u}}_k^{\,n}+\Delta t^2\sum_{i=1}^{s}\bar{B}_i(\lambda_k^2)f\big(\widehat{u_M^{ni}(x)}\big)_k,\\ \widehat{\dot{u}}_k^{\,n+1}=-\Delta t\beta_k^2\phi_1(\lambda_k^2)\widehat{u}_k^{\,n}+\phi_0(\lambda_k^2)\widehat{\dot{u}}_k^{\,n}+\Delta t\sum_{i=1}^{s}B_i(\lambda_k^2)f\big(\widehat{u_M^{ni}(x)}\big)_k,\\ \widehat{u}_k^{\,ni}=\phi_0(c_i^2\lambda_k^2)\widehat{u}_k^{\,n}+c_i\Delta t\phi_1(c_i^2\lambda_k^2)\widehat{\dot{u}}_k^{\,n}+\Delta t^2\sum_{j=1}^{s}A_{ij}(\lambda_k^2)f\big(\widehat{u_M^{nj}(x)}\big)_k,\\ \quad i=1,2,\cdots,s,\quad k=-M/2,\cdots,M/2-1,\end{cases}\tag{3.67}$$

with the Butcher tableau:

$$\begin{array}{c|c}\mathrm{c} & A(\lambda_k^2)\\ \hline & \bar{B}^{\mathsf{T}}(\lambda_k^2)\\ \hline & B^{\mathsf{T}}(\lambda_k^2)\end{array}=\begin{array}{c|ccc}c_1 & A_{11}(\lambda_k^2) & A_{12}(\lambda_k^2) & \cdots & A_{1s}(\lambda_k^2)\\ c_2 & A_{21}(\lambda_k^2) & A_{22}(\lambda_k^2) & \cdots & A_{2s}(\lambda_k^2)\\ \vdots & \vdots & \vdots & & \vdots\\ c_s & A_{s1}(\lambda_k^2) & A_{s2}(\lambda_k^2) & \cdots & A_{ss}(\lambda_k^2)\\ \hline & \bar{B}_1(\lambda_k^2) & \bar{B}_2(\lambda_k^2) & \cdots & \bar{B}_s(\lambda_k^2)\\ \hline & B_1(\lambda_k^2) & B_2(\lambda_k^2) & \cdots & B_s(\lambda_k^2)\end{array},$$

iteration is needed for practical application. In this chapter, we use the waveform relaxation iteration, which can be split into the following two phases.

I. Iteration procedure:

$$\begin{cases} \widehat{u}_{k,[0]}^{ni} = \phi_0(c_i^2\lambda_k^2)\widehat{u}_k^n + c_i\Delta t\phi_1(c_i^2\lambda_k^2)\widehat{\dot{u}}_k^n, \\ \widehat{u}_{k,[l+1]}^{ni} = \phi_0(c_i^2\lambda_k^2)\widehat{u}_k^n + c_i\Delta t\phi_1(c_i^2\lambda_k^2)\widehat{\dot{u}}_k^n + \Delta t^2\sum_{j=1}^{s} A_{ij}(\lambda_k^2)\widehat{f\left(u_{M,[l]}^{nj}(x)\right)}_k, \\ i = 1, 2, \cdots, s, \quad k = -M/2, \cdots, M/2-1, \quad l = 1, 2, \cdots. \end{cases} \tag{3.68}$$

For any error tolerance $\varepsilon > 0$, if the condition

$$\|u_{M,[l+1]}^{ni} - u_{M,[l]}^{ni}\|_{L^2} \leqslant \varepsilon$$

is satisfied, we define

$$u_M^{ni}(x) := u_{M,[l+1]}^{ni}(x) = \sum_{k=-M/2}^{M/2-1} \widehat{u}_{k,[l+1]}^{ni} \mathrm{e}^{\mathrm{i}kx}.$$

II. Output procedure:

$$\begin{cases} \widehat{u}_k^{n+1} = \phi_0(\lambda_k^2)\widehat{u}_k^n + \Delta t\phi_1(\lambda_k^2)\widehat{\dot{u}}_k^n + \Delta t^2\sum_{i=1}^{s} \bar{B}_i(\lambda_k^2)\widehat{f\left(u_M^{ni}(x)\right)}_k, \\ \widehat{\dot{u}}_k^{n+1} = -\Delta t\beta_k^2\phi_1(\lambda_k^2)\widehat{u}_k^n + \phi_0(\lambda_k^2)\widehat{\dot{u}}_k^n + \Delta t\sum_{i=1}^{s} B_i(\lambda_k^2)\widehat{f\left(u_M^{ni}(x)\right)}_k, \end{cases} \tag{3.69}$$

and define

$$u_M^{n+1}(x) = \sum_{k=-M/2}^{M/2-1} \widehat{u}_k^{n+1}\mathrm{e}^{\mathrm{i}kx}, \quad \dot{u}_M^{n+1}(x) = \sum_{k=-M/2}^{M/2-1} \widehat{\dot{u}}_k^{n+1}\mathrm{e}^{\mathrm{i}kx}.$$

In practice, the application of procedure (3.68)–(3.69) of the implicit ERKN-FS method could be understood as an explicit method. Therefore, if the solution $(u_M^n, \dot{u}_M^n) \in H_p^1(\Omega) \times L^2(\Omega)$ of the implicit ERKN-FS method satisfies

$$|||(u_M^n, \dot{u}_M^n)||| \leqslant K,$$

we then obtain

$$\|u_{M,[l]}^{ni}\|_{L^2} \leqslant (1+\Delta t)^{l+1}K \lesssim 1, \quad i = 1, 2, \cdots, s. \tag{3.70}$$

In a similar way to the proof of Theorem 3.7, we can deduce the boundedness for the implicit ERKN-FS methods (3.55)–(3.67).

Theorem 3.8 (Boundedness for a Single Time Step: Implicit ERKN-FS Methods) *Let the weights $\bar{B}_i(\lambda_k^2)$, $B_i(\lambda_k^2)$ and $A_{ij}(\lambda_k^2)$ of the implicit ERKN-FS method (3.55)–(3.67) satisfy the r-th order conditions (3.32). There exists a sufficiently small $0 < \tau_0 \leqslant 1$ such that $\Delta t \leqslant \tau_0$. If the numerical solution $(u_M^n, \dot{u}_M^n) \in H_p^1(\Omega) \times L^2(\Omega)$ of the implicit ERKN-FS method satisfies $|||(u_M^n, \dot{u}_M^n)||| \leqslant K$, then we have*

$$\|u_M^{ni}\| \lesssim 1, \quad i = 1, 2, \cdots, s,$$

and $(u_M^{n+1}, \dot{u}_M^{n+1}) \in H_p^1(\Omega) \times L^2(\Omega)$ with

$$\|u_M^{n+1}\|_{H^1} \leqslant \widetilde{C}_K \quad \text{and} \quad \|\dot{u}_M^{n+1}\|_{L^2} \leqslant \widetilde{C}_K,$$

where $\widetilde{C}_K$ is independent of the time stepsize Δt and spatial mesh size M.

According to the conclusion in Theorem 3.7 and Theorem 3.8 and using mathematical induction, suitable smoothness assumptions for the initial values $\varphi_1(\cdot)$ and $\varphi_2(\cdot)$ yield the boundedness of numerical solutions over a long-time interval $[t_0, T]$.

Theorem 3.9 *Assume that the weights $\bar{B}_i(\lambda_k^2)$, $B_i(\lambda_k^2)$ and $A_{ij}(\lambda_k^2)$ of the ERKN-FS method (3.55)–(3.56) satisfy the r-th order conditions (3.32). There exists a sufficiently small $0 < \tau_0 \leqslant 1$ such that $\Delta t \leqslant \tau_0$. If the initial conditions $\big(\varphi_1(x), \varphi_2(x)\big) \in H_p^1(\Omega) \times L^2(\Omega)$ satisfy $|||(\varphi_1, \varphi_2)||| \leqslant K_0$, then we have $(u_M^n, \dot{u}_M^n) \in H_p^1(\Omega) \times L^2(\Omega)$ with*

$$|||(u_M^{n+1}, \dot{u}_M^{n+1})||| \leqslant C_{K_0} \quad \text{and} \quad \|u_M^{ni}\|_{L^2} \leqslant C_{K_0}, \quad i = 1, 2, \cdots, s,$$

where C_{K_0} is independent of the time stepsize Δt and spatial mesh size M.

Proof By mathematical induction, the proof of the theorem is quite similar to Theorem 3.7 and Theorem 3.8, we omit the details here for brevity. □

Using the boundedness of numerical solutions, we will analyse the error bounds for the ERKN-FS methods. To this end, we introduce the modified H^1-norm and modified energy norm:

$$|[u_M]|_{H^1} = \left(\sum_{k=-M/2}^{M/2-1} (\rho + \varepsilon^2 k^2) |\hat{u}_k|^2 \right)^{1/2} \quad \text{and} \quad |||[(u_M, \dot{u}_M)]||| = \sqrt{|[u_M]|_{H^1}^2 + \|\dot{u}_M\|_{L^2}^2}.$$

Obviously, the modified H^1-norm is equivalent to the normal H^1-norm, namely

$$\min\{\sqrt{\rho}, \varepsilon\} \, \|u_M\|_{H^1} \leqslant |[u_M]|_{H^1} \leqslant \max\{\sqrt{\rho}, \varepsilon\} \, \|u_M\|_{H^1}. \tag{3.71}$$

We also assume that the weights $\bar{B}_i(\lambda_k^2)$, $B_i(\lambda_k^2)$ and $A_{ij}(\lambda_k^2)$ satisfy the r-th order conditions and the nonlinear function $f(\cdot)$ satisfies $\partial_t^r f \in L^\infty\big([t_0, T], L^2(\Omega)\big)$. Then the error system of ERKN-FS methods is to find $e_M^n(x)$, $\dot{e}_M^n(x)$ and $e_M^{ni}(x)$ in the space X_M, i.e.,

$$e_M^{n+1}(x) = \sum_{k=-M/2}^{M/2-1} \widehat{e}_k^{\,n+1} \mathrm{e}^{\mathrm{i}kx}, \quad \dot{e}_M^{n+1}(x) = \sum_{k=-M/2}^{M/2-1} \widehat{\dot{e}}_k^{\,n+1} \mathrm{e}^{\mathrm{i}kx}, \quad e_M^{ni}(x) = \sum_{k=-M/2}^{M/2-1} \widehat{e}_k^{\,ni} \mathrm{e}^{\mathrm{i}kx} \tag{3.72}$$

such that

$$\begin{cases} \widehat{e}_k^{\,n+1} = \phi_0(\lambda_k^2)\widehat{e}_k^{\,n} + \Delta t \phi_1(\lambda_k^2)\widehat{\dot{e}}_k^{\,n} + \Delta t^2 \sum_{i=1}^{s} \bar{B}_i(\lambda_k^2) \Delta \widehat{f}_k^{\,ni} + \widehat{\delta}_k^{\,n+1}, \\ \widehat{\dot{e}}_k^{\,n+1} = -\Delta t \beta_k^2 \phi_1(\lambda_k^2)\widehat{e}_k^{\,n} + \phi_0(\lambda_k^2)\widehat{\dot{e}}_k^{\,n} + \Delta t \sum_{i=1}^{s} B_i(\lambda_k^2) \Delta \widehat{f}_k^{\,ni} + \widehat{\dot{\delta}}_k^{\,n+1}, \\ \widehat{e}_k^{\,ni} = \phi_0(c_i^2\lambda_k^2)\widehat{e}_k^{\,n} + c_i \Delta t \phi_1(c_i^2\lambda_k^2)\widehat{\dot{e}}_k^{\,n} + \Delta t^2 \sum_{j=1}^{s} A_{ij}(\lambda_k^2) \Delta \widehat{f}_k^{\,nj} + \widehat{\Delta}_k^{\,ni}, \\ i = 1, 2, \cdots, s, \quad k = -M/2, \cdots, M/2 - 1. \end{cases} \tag{3.73}$$

where $\Delta \widehat{f}_k^{\,ni} = \widehat{f(u)_k}(t_n + c_i \Delta t) - \widehat{f\big(u_M^{ni}\big)_k}$ and the remainders $\widehat{\delta}_k^{\,n+1}$, $\widehat{\dot{\delta}}_k^{\,n+1}$ and $\widehat{\Delta}_k^{\,ni}$ can be represented as

$$\begin{aligned} \widehat{\delta}_k^{\,n+1} = & \sum_{l=0}^{r-1} \Delta t^{k+2} \left(\phi_{k+2}(\lambda_k^2) - \sum_{i=1}^{s} \bar{B}_i(\lambda_k^2) \frac{c_i^k}{k!} \right) \frac{\mathrm{d}^l}{\mathrm{d}t^l} \widehat{f(u)_k}(t_n) \\ & + \Delta t^{r+2} \int_0^1 (1-z) \phi_1\big((1-z)^2\lambda_k^2\big) \int_0^z \frac{(z-\tau)^{r-1}}{(r-1)!} \frac{\mathrm{d}^r}{\mathrm{d}t^r} \widehat{f(u)_k}(t_n + \tau \Delta t) \mathrm{d}\tau \mathrm{d}z \\ & - \Delta t^{r+2} \sum_{i=1}^{s} \bar{B}_i(\lambda_k^2) \int_0^{c_i} \frac{(c_i - \tau)^{r-1}}{(r-1)!} \frac{\mathrm{d}^r}{\mathrm{d}t^r} \widehat{f(u)_k}(t_n + \tau \Delta t) \mathrm{d}\tau, \end{aligned} \tag{3.74}$$

$$\begin{aligned} \widehat{\dot{\delta}}_k^{\,n+1} = & \sum_{k=0}^{r-1} \Delta t^{k+1} \left(\phi_{k+1}(\lambda_k^2) - \sum_{i=1}^{s} B_i(\lambda_k^2) \frac{c_i^k}{k!} \right) \frac{\mathrm{d}^l}{\mathrm{d}t^l} \widehat{f(u)_k}(t_n) \\ & + \Delta t^{r+1} \int_0^1 \phi_0\big((1-z)^2\lambda_k^2\big) \int_0^z \frac{(z-\tau)^{r-1}}{(r-1)!} \frac{\mathrm{d}^r}{\mathrm{d}t^r} \widehat{f(u)_k}(t_n + \tau \Delta t) \mathrm{d}\tau \mathrm{d}z \\ & - \Delta t^{r+1} \sum_{i=1}^{s} B_i(\lambda_k^2) \int_0^{c_i} \frac{(c_i - \tau)^{r-1}}{(r-1)!} \frac{\mathrm{d}^r}{\mathrm{d}t^r} \widehat{f(u)_k}(t_n + \tau \Delta t) \mathrm{d}\tau, \end{aligned} \tag{3.75}$$

and

$$\begin{aligned}\widehat{\Delta}_k^{ni} =& \sum_{k=0}^{r-1} \Delta t^{k+2} \left(c_i^{k+2} \phi_{k+2}(c_i^2 \lambda_k^2) - \sum_{j=1}^{s} A_{ij}(\lambda_k^2) \frac{c_j^k}{k!} \right) \frac{\mathrm{d}^l}{\mathrm{d}t^l} \widehat{f(u)_k}(t_n) \\ &+ c_i^{r+2} \Delta t^{r+2} \int_0^1 (1-z) \phi_1\big((1-z)^2 c_i^2 \lambda_k^2\big) \int_0^z \frac{(z-\tau)^{r-1}}{(r-1)!} \frac{\mathrm{d}^r}{\mathrm{d}t^r} \widehat{f(u)_k}(t_n + \tau c_i \Delta t) \mathrm{d}\tau \mathrm{d}z \\ &- \Delta t^{r+2} \sum_{i=1}^{s} A_{i,j}(\lambda_k^2) \int_0^{c_j} \frac{(c_j-\tau)^{r-1}}{(r-1)!} \frac{\mathrm{d}^r}{\mathrm{d}t^r} \widehat{f(u)_k}(t_n + \tau \Delta t) \mathrm{d}\tau. \end{aligned} \tag{3.76}$$

Using energy techniques, we can obtain the convergence result for the ERKN-FP methods.

Theorem 3.10 ($H^1 \times L^2$ **Error Bounds of the ERKN-FP Method**) *Let u^n, $\dot{u}^n$ and u^{ni} be the approximations obtained from the ERKN-FP method (3.57)–(3.58), and the weights $\bar{B}_i(\lambda_k^2)$, $B_i(\lambda_k^2)$ and $A_{ij}(\lambda_k^2)$ satisfy the r-th order conditions (3.32). Then, under the assumption of Theorem 3.9, there exist two sufficiently small constants $0 < \tau_0 \leqslant 1$ and $0 < h_0 \leqslant 1$, such that*

$$\|u(\cdot, t_n) - (I_M u^n)(\cdot)\|_{H^1} + \|u_t(\cdot, t_n) - (I_M \dot{u}^n)(\cdot)\|_{L^2} \lesssim \Delta t^r + \Delta x^{m_0},$$

when $0 < \Delta t \leqslant \tau_0$ and $0 < \Delta x \leqslant h_0$.

Proof According to Lemma 3.5, it is easy to obtain the following estimates for the remainders $\widehat{\delta}_k^{n+1}$, $\widehat{\dot{\delta}}_k^{n+1}$ and $\widehat{\Delta}_k^{ni}$:

$$|[\delta_M^{n+1}]|_{H^1} \leqslant K_3 \Delta t^{r+1}, \quad \|\dot{\delta}_M^{n+1}\|_{L^2} \leqslant K_3 \Delta t^{r+1}, \quad \sum_{i=1}^{s} \|\Delta_M^{ni}\|_{L^2} \leqslant K_3 \Delta t^{r+2},$$

where the constant K_3 is dependent on K_2, B, $\hat{B}$, $\bar{B}$ and β, but independent of the time stepsize Δt and the spatial mesh size M. Rewriting the first two equations in (3.73) as

$$\begin{bmatrix} \beta_k \widehat{e}_k^{n+1} \\ \widehat{\dot{e}}_k^{n+1} \end{bmatrix} = \Omega(1, 0, \lambda_k^2) \begin{bmatrix} \beta_k \widehat{e}_k^{n} \\ \widehat{\dot{e}}_k^{n} \end{bmatrix} + \Delta t \sum_{i=1}^{s} \begin{bmatrix} \beta_k \bar{B}_i(\lambda_k^2) \Delta \widehat{f}_k^{ni} \\ B_i(\lambda_k^2) \Delta \widehat{f}_k^{ni} \end{bmatrix} + \begin{bmatrix} \beta_k \widehat{\delta}_k^{n+1} \\ \widehat{\dot{\delta}}_k^{n+1} \end{bmatrix},$$

by taking the l_2 inner product on both sides and using the Cauchy inequality, we have

$$\beta_k^2|\,\widehat{e}_k^{\,n+1}|^2+|\,\widehat{\dot{e}}_k^{\,n+1}|^2 \leqslant \big(1+\Delta t(s+1)\big)\Big(\beta_k^2|\,\widehat{e}_k^{\,n}|^2+|\,\widehat{\dot{e}}_k^{\,n}|^2\Big)+3\Delta t(\hat{B}^2+B^2)\sum_{i=1}^{s}|\,\Delta\widehat{f}_k^{\,ni}\,|^2$$
$$+(2+\frac{1}{\Delta t})\Big(\beta_k^2|\widehat{\delta}_k^{\,n+1}|^2+|\widehat{\dot{\delta}}_k^{\,n+1}|^2\Big).$$

Summing up the above inequality for k from $-M/2$ to $M/2-1$ and using Parseval's identity yields

$$|||[(e_M^{n+1},\dot{e}_M^{n+1})]||^2 \leqslant \big(1+\Delta t(1+s)\big)|||[(e_M^{n},\dot{e}_M^{n})]||^2$$
$$+3\Delta t(\hat{B}^2+B^2)\sum_{i=1}^{s}\big\|f\big(u(\cdot,t_n+c_i\Delta t)\big)-f\big(u_M^{ni}\big)\big\|_{L^2}^2+4K_3\Delta t^{2r+1}. \tag{3.77}$$

It then follows from the conclusion of Theorem 3.9 and the assumptions for $f(\cdot)$ that

$$\begin{aligned}&\big\|f\big(u(\cdot,t_n+c_i\Delta t)\big)-f\big(u_M^{ni}\big)\big\|_{L^2}\\ =&\left\|\int_0^1 f'\Big(\tau u_M^{ni}+(1-\tau)u(\cdot,t_n+c_i\Delta t)\Big)\mathrm{d}\tau\cdot\big(u_M^{ni}(\cdot)-u(\cdot,t_n+c_i\Delta t)\big)\right\|_{L^2}\\ \leqslant& K_2\big\|u_M^{ni}(\cdot)-u(\cdot,t_n+c_i\Delta t)\big\|_{L^2}\leqslant K_2\Big(\big\|e_M^{ni}\big\|_{L^2}+\Delta x^{m_0+1}\Big).\end{aligned}$$

Hence, inserting the above inequality into (3.77), we have

$$|||[(e_M^{n+1},\dot{e}_M^{n+1})]||^2 \leqslant \big(1+(1+s)\Delta t\big)|||[(e_M^{n},\dot{e}_M^{n})]||^2+K_4\Delta t\sum_{i=1}^{s}\|e_M^{ni}\|_{L^2}^2$$
$$+K_5\Delta t\Big(\Delta t^{2r}+\Delta x^{2m_0+2}\Big), \tag{3.78}$$

where K_4 and K_5 are constants and independent of Δt and Δx. Clearly, to show the required error bounds, we need to estimate the term $\sum_{i=1}^{s}\|e_M^{ni}\|_{L^2}$. It follows from taking the L^2 norm on both sides of the third equation in (3.73) that

$$\|e_M^{ni}\|_{L^2}\leqslant\|e_M^{n}\|_{L^2}+\|\dot{e}_M^{n}\|_{L^2}+\Delta t^2\beta\sum_{i=1}^{s}\big\|f\big(u(\cdot,t_n+c_i\Delta t)\big)-f\big(u_M^{ni}\big)\big\|_{L^2}+\sum_{i=1}^{s}\|\Delta_M^{ni}\|_{L^2}$$
$$\leqslant|||[(e_M^{n},\dot{e}_M^{n})]||_{L^2}+\Delta t^2\beta K_2\sum_{i=1}^{s}\big(\big\|e_M^{ni}\big\|_{L^2}+\Delta x^{m_0+1}\big)+\sum_{i=1}^{s}\|\Delta_M^{ni}\|_{L^2}.$$

This, together with the assumption that the time stepsize satisfies $\Delta t \leqslant \sqrt{\frac{1}{2s\beta K_2}}$, implies

$$\sum_{i=1}^{s} \left\| e_M^{ni} \right\|_{L^2} \leqslant 2s|||[(e_M^n, \dot{e}_M^n)]|||_{L^2} + 2sK_3\Delta t^{r+2} + s\Delta x^{m_0+1}.$$

Inserting the result into (3.78) leads to

$$|||[(e_M^{n+1}, \dot{e}_M^{n+1})]|||^2 \leqslant \left(1 + K_6\Delta t\right)|||[(e_M^n, \dot{e}_M^n)]|||^2 + K_7\Delta t\Big(\Delta t^{2r} + \Delta x^{2m_0+2}\Big). \tag{3.79}$$

Applying Gronwall's inequality to (3.79) results in

$$|||[(e_M^{n+1}, \dot{e}_M^{n+1})]||| \lesssim \Delta t^r + \Delta x^{m_0+1}.$$

Since the modified H^1-norm is equivalent to the normal H^1-norm and the relation (3.59), we obtain

$$\|e^n\|_{H^1} + \|\dot{e}^n\|_{L^2} \lesssim \Delta t^r + \Delta x^{m_0}.$$

Theorem 3.10 is proved. □

Remark 3.3.1 It follows from the convergence analysis stated above that we gain an insight into the significance of the ERKN-FP methods. That is, the ERKN-FP methods are independent of the restriction between the time stepsize Δt and the spatial stepsize Δx. In other words, the ERKN-FP methods are free from the CFL condition. This is another important property of ERKN integrators when applied to the semilinear wave equation, which, unfortunately, is not shared by traditional schemes for PDEs in the literature.

3.4 Numerical Experiments

In this section, we present results of numerical experiments to verify our theoretical analysis for the ERKN time integrators. In order to demonstrate the superiority of ERKN time integrators, we select the following time integrators for comparison:

- ISV: the improved explicit symplectic Störmer–Verlet formula of order two given in [13];
- ERKN3s4: the three-stage symmetric and symplectic explicit ERKN method of order four (see [15]);
- IERKN2s4: the two-stage implicit symplectic ERKN method of order four;
- IERKN3s6: the three-stage implicit symplectic ERKN method of order six;

- SV: the classical explicit symplectic Strömer–Verlet formula of order two (see [8]);
- RKN3s4: the three-stage explicit symplectic RKN method of order four (see [8]);
- IRKN2s4: the two-stage implicit symplectic RKN method of order four (see [51]);
- IRKN3s6: the three-stage implicit symplectic RKN method of order six (see [51]).

Using the established mapping between the ERKN group and the RKN group (see [52]), it is known that ERKN methods with an arbitrarily high order can be obtained from the corresponding RKN methods. Hence, the IERKN2s4 method and the IERKN3s6 method are yielded by the well-known IRKN2s4 method and IRKN3s6 method, respectively. For implicit time integrators, we use fixed-point iteration and choose the tolerance as 10^{-15} and the maximum iteration number as 100. Here, it is noted that when the error of a method under consideration is very large for some Δt, we do not plot the corresponding points in the efficiency curves in the numerical experiments. The efficiency curves are given as the log-log plots of the errors.

Problem 3.1 We consider the Duffing equation

$$\begin{cases} \ddot{q} + \omega^2 q = k^2(2q^3 - q), \\ q(0) = 0, \quad \dot{q}(0) = \omega, \end{cases}$$

where $0 \leqslant k < \omega$. This is a Hamiltonian system with the conservation of the following Hamiltonian

$$H\big(q(t), \dot{q}(t)\big) = \frac{1}{2}\dot{q}(t)^2 + \frac{1}{2}\omega^2 q(t)^2 + \frac{k^2}{2}\big(q(t)^2 - q(t)^4\big).$$

The analytic solution of the Duffing equation is well known, and given by

$$q(t) = sn(\omega t, k/\omega),$$

where sn means the Jacobian elliptic function. Obviously, the analytic solution $q(t)$ satisfies $|q(t)| \leqslant 1$, i.e., $q^2 \geqslant q^4$. Therefore, for each $\omega > 0$ (no matter how big ω is) there exists a constant K such that

$$\frac{1}{2}\dot{q}(t)^2 + \frac{1}{2}\omega^2 q(t)^2 \leqslant H\big(q(0), \dot{q}(0)\big) \leqslant \frac{K^2}{2}.$$

Then, the finite-energy condition (3.23) is verified. We choose $k = 0.03$ and different frequencies $\omega = 5, 10$ and 20 which are similar to those in [53]. We integrate the Problem 3.1 on the interval [0, 1000] to verify our error estimates for the ISV method, the ERKN3s4 method, the IERKN2s4 method and the IERKN3s6

Table 3.1 Temporal accuracy of the "ISV" method for solving Problem 3.1 with different ω and Δt up to $T = 1000$

	Δt				
ω	$\Delta t_0 = 0.08$	$\Delta t_0/2$	$\Delta t_0/2^2$	$\Delta t_0/2^3$	$\Delta t_0/2^4$
$\omega = 5$	3.6227E − 7	8.4317E − 8	2.0714E − 8	5.1545E − 9	1.2843E − 9
Rate	*	2.1032	2.0252	2.0067	2.0048
$\omega = 10$	4.0951E − 7	7.1460E − 8	1.6455E − 8	4.0277E − 9	9.9857E − 10
Rate	*	2.5187	2.1186	2.0305	2.0120
$\omega = 20$	1.2973E − 5	9.1229E − 8	1.5503E − 8	3.5447E − 9	8.5937E − 10
Rate	*	–	2.5569	2.1288	2.0443

Table 3.2 Temporal accuracy of the "ERKN3s4" method for solving Problem 3.1 with different ω and Δt up to $T = 1000$

	Δt			
ω	$\Delta t_0 = 0.08$	$\Delta t_0/2$	$\Delta t_0/2^2$	$\Delta t_0/2^3$
$\omega = 5$	4.4048E − 8	2.7520E − 9	1.7404E − 10	1.3915E − 11
Rate	*	4.0005	3.9830	3.6447
$\omega = 10$	1.1427E − 7	6.5012E − 9	4.0112E − 10	3.0784E − 11
Rate	*	4.1356	4.0186	3.7038
$\omega = 20$	6.2331E − 6	2.0477E − 8	1.0892E − 9	7.1579E − 11
Rate	*	8.2498	4.2327	3.9276

Table 3.3 Temporal precision of the "IERKN2s4" method for solving Problem 3.1 with different ω and Δt up to $T = 1000$

	Δt				
ω	$\Delta t_0 = 0.1$	$\Delta t_0/2$	$\Delta t_0/2^2$	$\Delta t_0/2^3$	$\Delta t_0/2^4$
$\omega = 5$	1.9339E − 6	1.2139E − 7	7.6054E − 9	4.7731E − 10	3.0324E − 11
Rate	*	3.9938	3.9964	3.9940	3.9764
$\omega = 10$	1.5263E − 5	9.6938E − 7	6.0899E − 8	3.8101E − 9	2.4023E − 10
Rate	*	3.9768	3.9926	3.9985	3.9873
$\omega = 20$	1.1468E − 4	7.6411E − 6	4.8518E − 7	3.0467E − 8	1.9073E − 9
Rate	*	3.9077	3.9772	3.9932	3.9976

method with the different frequencies. The results in Tables 3.1 and 3.2 indicate that the convergence order of the ISV method and the ERKN3s4 method are of order two and order four, respectively. Tables 3.3 and 3.4 demonstrate that the IERKN2s4 method and the IERKN3s6 method are of order four and order six, respectively. The computational results are coincide with our theoretical analysis results.

The logarithm of the global errors GE$= \|q_N - q(1000)\|_2$ against different stepsizes for Problem 3.1 are plotted in Fig. 3.1. The logarithm of the global errors against different frequencies ω are displayed in Fig. 3.2. It can be observed from Fig. 3.2 that the ERKN integrators are independent of the frequency ω, whereas other traditional integrators depend on the frequency. In conclusion, Figs. 3.1

Table 3.4 Temporal precision of the "IERKN3s6" method for solving Problem 3.1 with different ω and Δt up to $T = 1000$

	Δt				
ω	$\Delta t_0 = 0.4$	$\Delta t_0/2$	$\Delta t_0/2^2$	$\Delta t_0/2^3$	$\Delta t_0/2^4$
$\omega = 5$	1.3355E − 5	2.2286E − 7	3.4864E − 9	5.6017E − 11	3.4615E − 12
Rate	*	5.9051	5.9983	5.9597	4.0164
$\omega = 10$	3.3252E − 4	6.5535E − 6	1.0957E − 7	1.7381E − 9	2.8857E − 10
Rate	*	5.6650	5.9024	5.9782	5.9124
$\omega = 20$	4.0302E − 3	1.6588E − 4	3.2996E − 6	5.4632E − 8	8.6855E − 9
Rate	*	4.6026	5.6517	5.9164	5.9750

and 3.2 demonstrate that the ERKN time integrators are much more superior to the traditional numerical methods in the literature.

Problem 3.2 We consider the nonlinear KG equation (see, e.g. [5, 29])

$$u_{tt}(x,t) - a^2 \Delta u(x,t) + a u(x,t) - b u^3(x,t) = 0,$$

in the region $(x,t) \in [-20, 20] \times [0, 10]$ with the initial conditions

$$u(x,0) = \sqrt{\frac{2a}{b}} \operatorname{sech}(\lambda x), \qquad u_t(x,0) = c\lambda \sqrt{\frac{2a}{b}} \operatorname{sech}(\lambda x) \tanh(\lambda x),$$

where $\lambda = \sqrt{a/(a^2 - c^2)}$ and $a, b, a^2 - c^2 > 0$. The exact solution of Problem 3.2 is given by

$$u(x,t) = \sqrt{\frac{2a}{b}} \operatorname{sech}(\lambda(x - ct)).$$

The real parameter $\sqrt{2a/b}$ represents the amplitude of a soliton which travels with velocity c. We use the parameters $a = 0.3$, $b = 1$ and $c = 0.25$ which are similar to those in [5, 29]. We integrate Problem 3.2 by using the IERKN3s6 time integrator with Fourier pseudospectral spatial discretisation (IERKN3s6-FP). The error graphs are shown in Fig. 3.3, with fixed time stepsize $\Delta t = 0.01$ and several values of spatial mesh size M. Numerical results demonstrate the spectral accuracy of the spatial discretisation.

In Tables 3.5 and 3.6, we fixed the spatial mesh size $M = 800$ and integrate the Problem 3.2 with different time stepsizes Δt to compute the temporal convergence order. The results demonstrate that the temporal accuracy is completely consistent with our theoretical analysis. In Fig. 3.4, we plot the logarithms of the global error $\mathrm{GE} = \|U(\Delta t; T) - u(\cdot, T)\|_2$ against different time stepsizes, where $U(\Delta t; T)$ denotes the numerical solution at time T with the time stepsize Δt. The results illustrate that the ERKN time integrators have much better precision than the RKN time integrators.

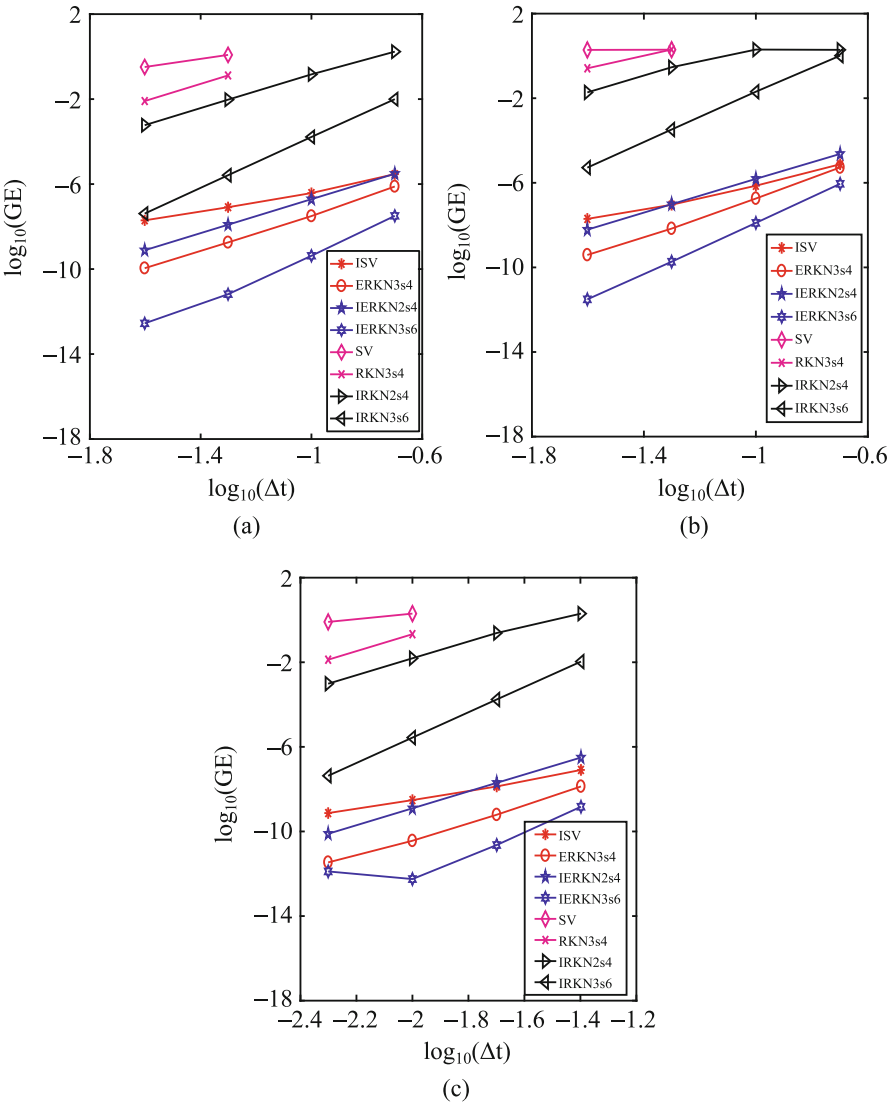

Fig. 3.1 Efficiency curves for Problem 3.1: The logarithm of the global errors GE $= \|q_N - q(1000)\|_2$ against different time stepsizes with frequencies $\omega = 5$ (**a**), 10 (**b**) and 20 (**c**)

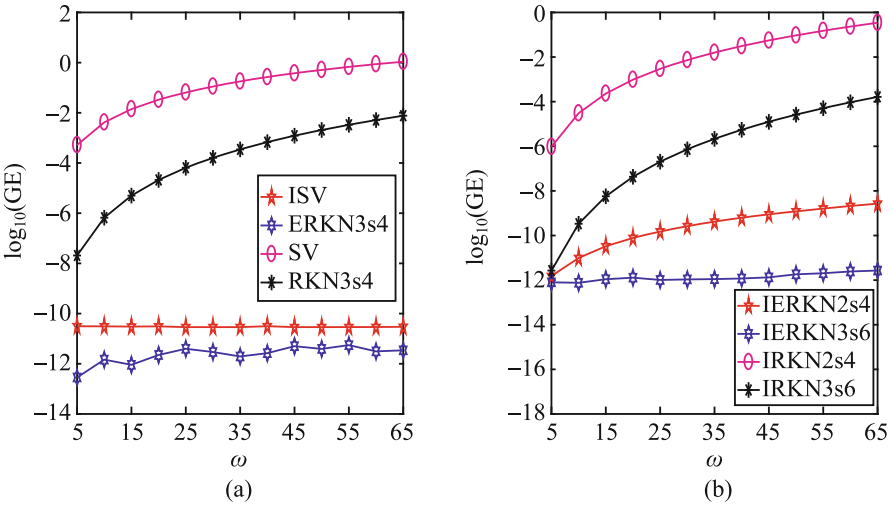

Fig. 3.2 Results of Problem 3.1: The logarithm of the global errors (GE) against different frequencies ω. (**a**) $\Delta t = 0.001$. (**b**) $\Delta t = 0.005$

Problem 3.3 Consider the nonlinear KG equation in the nonrelativistic limit regime (see [54, 55]):

$$\begin{cases} \varepsilon^2 u_{tt}(x,t) - \Delta u(x,t) + \dfrac{1}{\varepsilon^2} u(x,t) + f\big(u(x,t)\big) = 0, \\ u(x,0) = \psi_1(x), \quad u_t(x,0) = \dfrac{1}{\varepsilon^2}\psi_2(x), \end{cases} \tag{3.80}$$

in the region $(x,t) \in [-30,30] \times [0,T]$ with the initial functions

$$\psi_1(x) = 2\mathrm{e}^{-x^2}, \quad \psi_2(x) = 3\mathrm{e}^{-x^2}$$

and the cubic nonlinearity, i.e. $f(u) = u^3$. Here $0 < \varepsilon \ll 1$ is a dimensionless parameter which is inversely proportional to the speed of light, ψ_1 and ψ_2 are two given pieces of real-valued initial data which are independent of ε. We simulate the experiment by using the IERKN3s6-FP method with the time stepsize $\Delta t = 10^{-4}$ and spatial mesh size $M = 1200$. The simulation results are displayed in Figs. 3.5 and 3.6. Obviously, the problem is highly oscillatory in time with respect to different values of parameter ε.

To test the temporal accuracy of the time integrators "ISV", "ERKN3s4", "IERKN2s4" and "IERKN3s6", we fixed the spatial mesh size as $M = 1200$. As is known, the exact solution of the Problem 3.3 cannot be represented explicitly. Therefore, we use a posterior error estimate, i.e. RE $= \|U(\Delta t; T) - U(\Delta t/2; T)\|_2$, to compute the convergence order. The computational results are

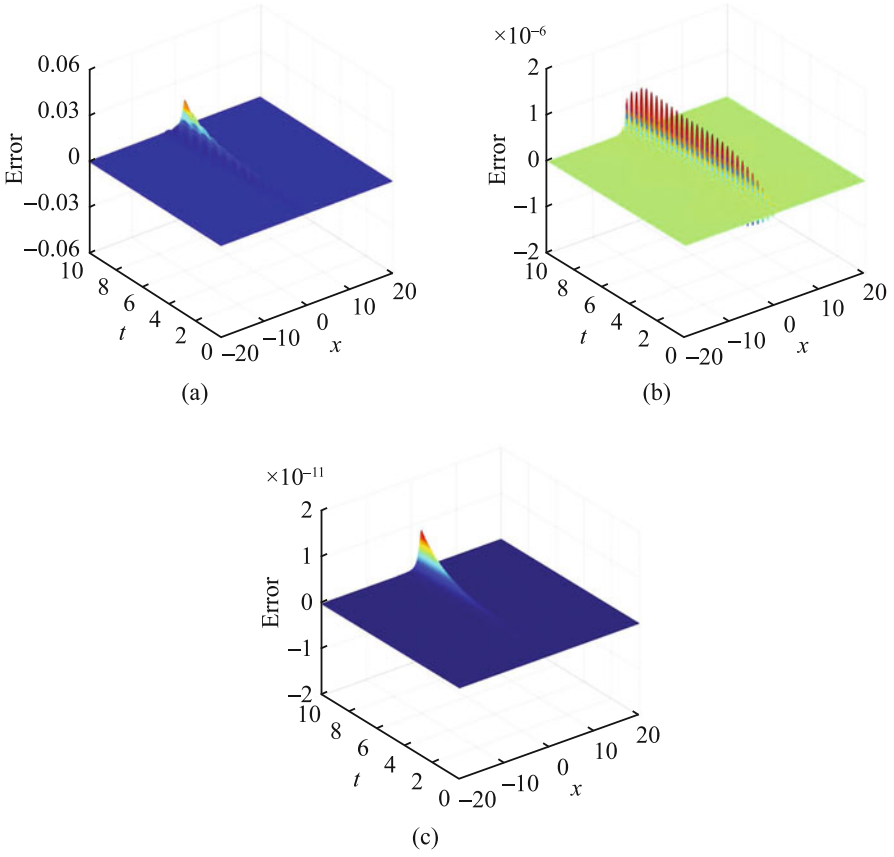

Fig. 3.3 The errors for Problem 3.2 obtained by using the IERKN3s6-FP method for $\Delta t = 0.01$ with (**a**) $M = 200$, (**b**) $M = 400$, and (**c**) $M = 800$

Table 3.5 Temporal precision of "ISV" and "ERKN3s4" methods for solving Problem 3.2 with different Δt up to $T = 10$ ($\Delta t_0 = 0.1$)

	ISV		ERKN3s4	
	Global error	Rate	Global error	Rate
Δt_0	1.2884E − 1	*	6.9442E − 4	*
$\Delta t_0/2$	3.3095E − 2	1.9609	4.3965E − 5	3.9814
$\Delta t_0/2^2$	8.3311E − 3	1.9900	2.7567E − 6	3.9953
$\Delta t_0/2^3$	2.0864E − 3	1.9975	1.7244E − 7	3.9988

Table 3.6 Temporal precision of "IERKN2s4" and "IERKN3s6" methods for solving Problem 3.2 with different Δt up to $T = 10$ ($\Delta t_0 = 0.4$)

	IERKN2s4		IERKN3s6	
	Global error	Rate	Global error	Rate
Δt_0	1.4215E − 3	*	9.0669E − 6	*
$\Delta t_0/2$	9.0773E − 5	3.9690	1.4335E − 7	5.9830
$\Delta t_0/2^2$	5.7039E − 6	3.9922	2.2590E − 9	5.9877
$\Delta t_0/2^3$	3.5696E − 7	3.9981	1.7062E − 11	7.0488

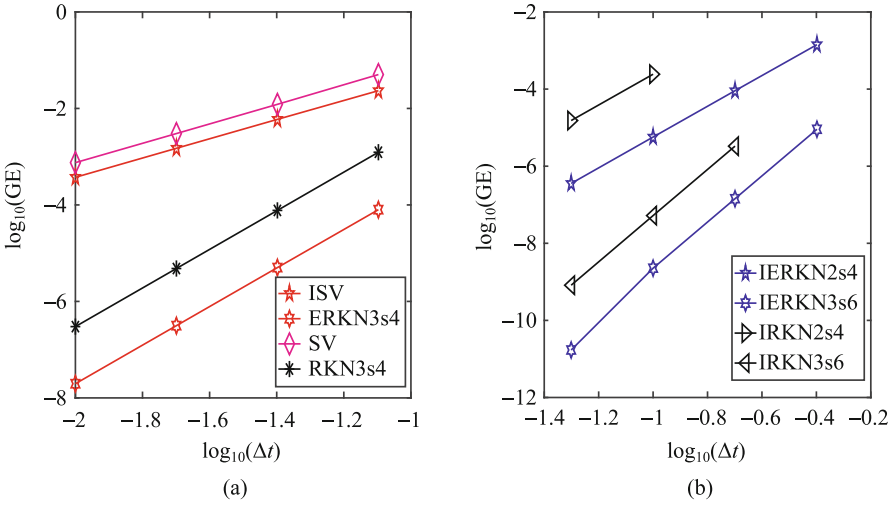

Fig. 3.4 Efficiency curves for Problem 3.2: The logarithm of the errors GE $= \|U(\Delta t; T) - u(\cdot, T)\|_2$ against different time stepsizes. (**a**) Explicit methods. (**b**) Implicit methods

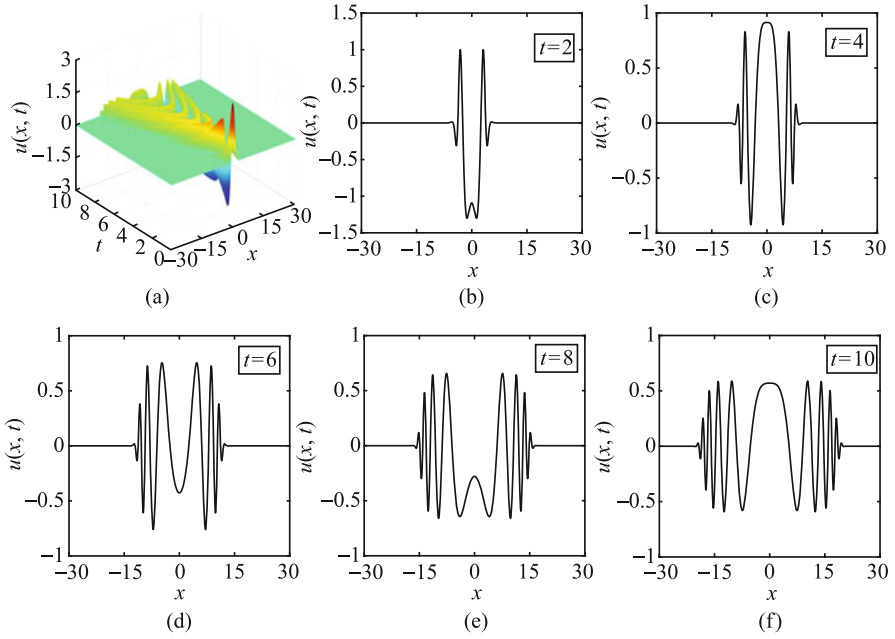

Fig. 3.5 The graphs of Problem 3.3 obtained by using the IERKN3s6-FP method for $\varepsilon = 0.5$, $\Delta t = 10^{-4}$ and $\Delta x = 1/20$. (**a**) $\varepsilon = 0.5$, (**b**) $t = 2$, (**c**) $t = 4$, (**d**) $t = 6$, (**e**) $t = 8$, (**f**) $t = 10$

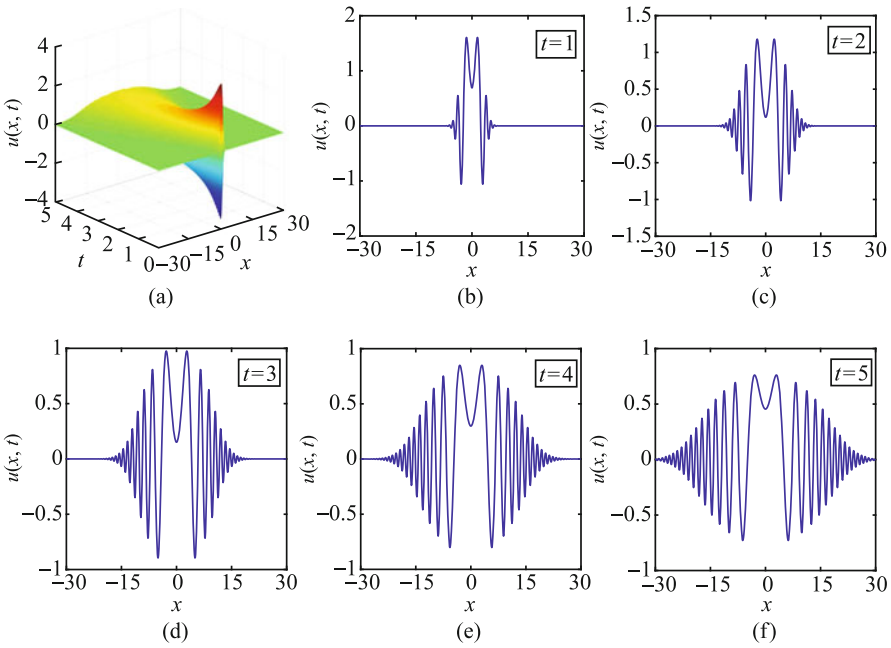

Fig. 3.6 The graphs of Problem 3.3 obtained by using the IERKN3s6-FP method for $\varepsilon = 0.1$, $\Delta t = 10^{-4}$ and $\Delta x = 1/20$. (**a**) $\varepsilon = 0.1$, (**b**) $t = 1$, (**c**) $t = 2$, (**d**) $t = 3$, (**e**) $t = 4$, (**f**) $t = 5$

Table 3.7 Temporal accuracy of the "ISV" method for solving Problem 3.3 with different ε and Δt at time $T = 2$

	Δt				
ε	$\Delta t_0 = 0.1$	$\Delta t_0/2$	$\Delta t_0/2^2$	$\Delta t_0/2^3$	$\Delta t_0/2^4$
$\varepsilon = 1$	4.1772E − 2	9.8027E − 3	2.4133E − 3	6.0104E − 4	1.5012E − 4
Rate	*	2.0913	2.0222	2.0055	2.0014
	$\Delta t_0 = 0.04$	$\Delta t_0/2$	$\Delta t_0/2^2$	$\Delta t_0/2^3$	$\Delta t_0/2^4$
$\varepsilon = 0.5$	3.8736E − 2	9.5530E − 3	2.3790E − 3	5.9416E − 4	1.4850E − 4
Rate	*	2.0196	2.0056	2.0014	2.0004
$\varepsilon = 0.1$	1.9373E − 2	5.1113E − 3	1.2885E − 3	3.2271E − 4	8.0712E − 5
Rate	*	1.9223	1.9880	1.9974	1.9994

listed in Tables 3.7, 3.8, 3.9 and 3.10 demonstrating that the temporal accuracy is completely consistent with our theoretical analysis.

In comparison with the corresponding time integrators "SV", "RKN3s4", "IRKN2s4" and "IRKN3s6", we fix the spatial mesh size as $M = 1200$ and integrate with different time stepsizes at time $T = 2$. The logarithms of the relative errors $\log_{10}(\text{RE})$ are plotted in Fig. 3.7. It can be observed from Fig. 3.7 that the ERKN time integrators are more accurate than these traditional methods.

Table 3.8 Temporal accuracy of the "ERKN3s4" method for solving Problem 3.3 with different ε and Δt at time $T = 2$

	Δt				
ε	$\Delta t_0 = 0.1$	$\Delta t_0/2$	$\Delta t_0/2^2$	$\Delta t_0/2^3$	$\Delta t_0/2^4$
$\varepsilon = 1$	4.0049E − 2	2.0521E − 3	1.2269E − 4	7.5856E − 6	4.7283E − 7
Rate	*	4.2866	4.0641	4.0156	4.0039
	$\Delta t_0 = 0.04$	$\Delta t_0/2$	$\Delta t_0/2^2$	$\Delta t_0/2^3$	$\Delta t_0/2^4$
$\varepsilon = 0.5$	4.3176E − 2	2.3654E − 3	1.4380E − 4	8.9274E − 6	5.5704E − 7
Rate	*	4.1900	4.0400	4.0096	4.0024
$\varepsilon = 0.1$	3.4882E − 2	2.2846E − 3	1.4431E − 4	9.0431E − 6	5.6556E − 7
Rate	*	3.9325	3.9847	3.9962	3.9991

Table 3.9 Temporal precision of the "IERKN2s4" method for solving Problem 3.3 with different ε and Δt at time $T = 2$

	Δt				
ε	$\Delta t_0 = 0.1$	$\Delta t_0/2$	$\Delta t_0/2^2$	$\Delta t_0/2^3$	$\Delta t_0/2^4$
$\varepsilon = 1$	2.3594E − 4	1.4193E − 5	8.8175E − 7	5.5037E − 8	3.4388E − 9
Rate	*	4.0551	4.0087	4.0019	4.0004
	$\Delta t_0 = 0.05$	$\Delta t_0/2$	$\Delta t_0/2^2$	$\Delta t_0/2^3$	$\Delta t_0/2^4$
$\varepsilon = 0.5$	6.5929E − 4	3.4212E − 5	2.0537E − 6	1.2721E − 7	7.9337E − 9
Rate	*	4.2683	4.0582	4.0129	4.0031
	$\Delta t_0 = 0.005$	$\Delta t_0/2$	$\Delta t_0/2^2$	$\Delta t_0/2^3$	$\Delta t_0/2^4$
$\varepsilon = 0.1$	2.1318E − 3	2.0379E − 4	1.3783E − 5	8.7673E − 7	5.5029E − 8
Rate	*	3.3869	3.8861	3.9746	3.9939

Table 3.10 Temporal precision of the "IERKN3s6" method for solving Problem 3.3 with different ε and Δt at time $T = 2$

	Δt				
ε	$\Delta t_0 = 0.1$	$\Delta t_0/2$	$\Delta t_0/2^2$	$\Delta t_0/2^3$	$\Delta t_0/2^4$
$\varepsilon = 1$	3.0107E − 6	3.5378E − 8	5.2866E − 10	8.1239E − 12	2.6356E − 13
Rate	*	6.4111	6.0644	6.0240	–
	$\Delta t_0 = 0.05$	$\Delta t_0/2$	$\Delta t_0/2^2$	$\Delta t_0/2^3$	$\Delta t_0/2^4$
$\varepsilon = 0.5$	2.3162E − 5	2.9908E − 7	4.5292E − 9	7.0507E − 11	1.2447E − 12
Rate	*	6.2751	6.0451	6.0053	5.8239
	$\Delta t_0 = 0.005$	$\Delta t_0/2$	$\Delta t_0/2^2$	$\Delta t_0/2^3$	$\Delta t_0/2^4$
$\varepsilon = 0.1$	4.3967E − 4	2.0432E − 6	3.0716E − 8	4.7584E − 10	6.6287E − 12
Rate	*	7.7494	6.0557	6.0124	6.1656

In Fig. 3.8, we use the numerical solution obtained by the sixth-order IERKN3s6-FP method with the very small time stepsize $\Delta t = 10^{-4}$ and the spatial mesh size $M = 1200$, as the reference solution of the exact solution. The logarithms of the global errors against different parameters are plotted in Fig. 3.8. The results again show that the ERKN time integrators for solving the highly oscillatory problems are much superior to the RKN time integrators.

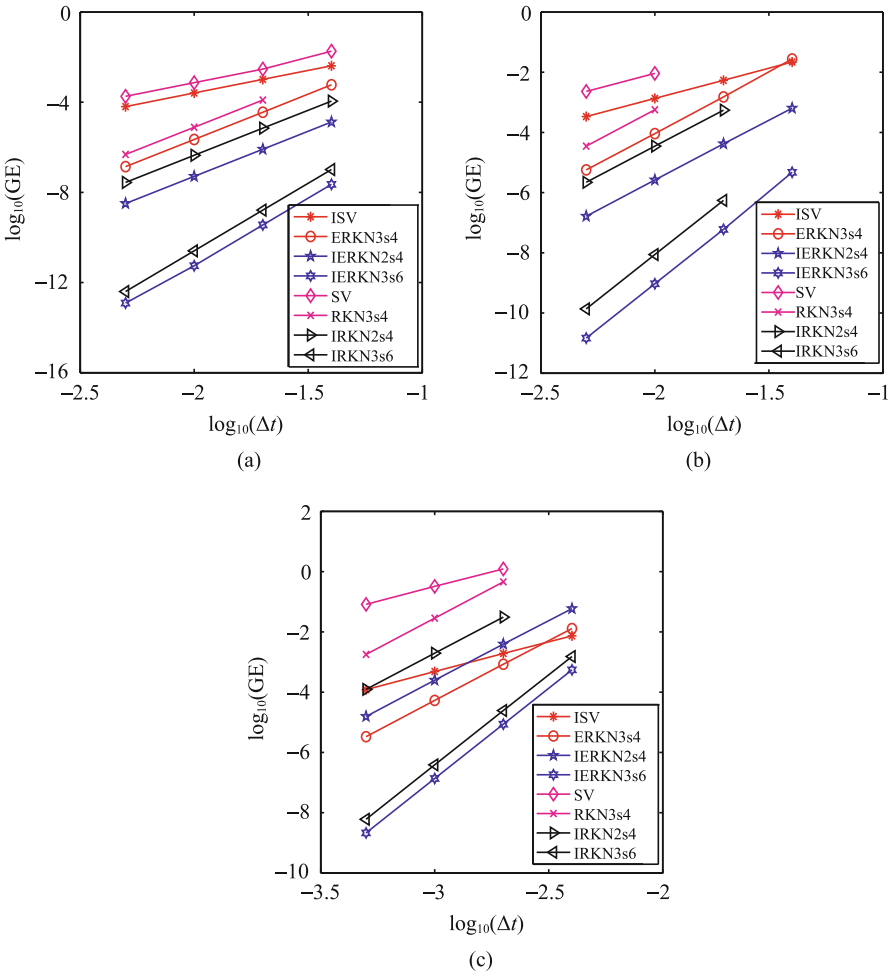

Fig. 3.7 Efficiency curves for Problem 3.3: The logarithm of the relative errors $\mathrm{RE} = \|U(\Delta t; T) - U(\Delta t/2; T)\|_2$ against different time stepsizes with parameters $\varepsilon = 1$ (**a**), 0.5 (**b**) and 0.1 (**c**)

3.5 Conclusions

In this chapter, we have made a comprehensive investigation on the nonlinear stability and convergence of ERKN integrators for solving the system of nonlinear multi-frequency highly oscillatory second-order ODEs (3.1) with a takanami number. On the basis of the finite-energy condition, it turns out that the nonlinear stability and the global error bounds are independent of the dominant frequency-matrix and the takanami number. Employing the energy technique, we also analysed

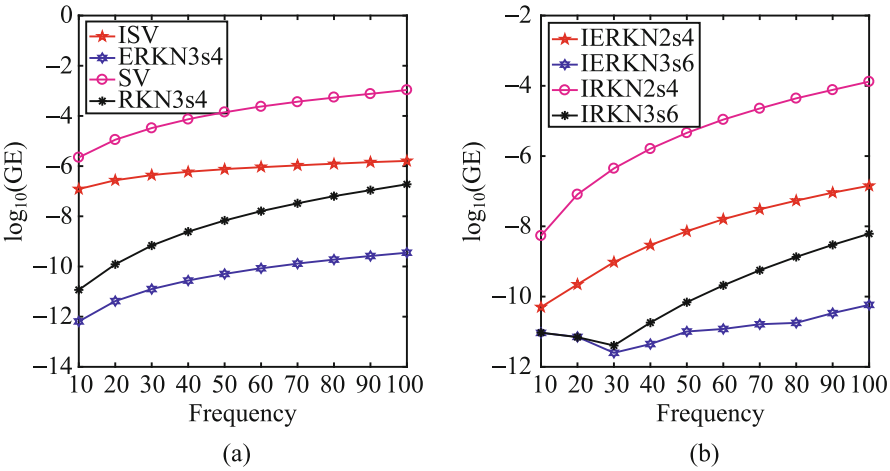

Fig. 3.8 Results of Problem 3.3: The logarithm of the global errors (GE) against different parameters $1/\varepsilon^2$. (**a**) $\Delta t = 0.001$. (**b**) $\Delta t = 0.005$

the convergence of the ERKN time integrators with the Fourier pseudospectral spatial discretisation when applied to semilinear wave equations. Another important issue is that the ERKN-FP method eliminates necessity for the CFL restriction, when applied to semilinear wave equations, whereas traditional schemes for solving PDEs suffer from this crucial restriction which greatly affects the efficiency of these schemes. This outstanding property of ERKN integrators ensures that an ERKN-type time integrator can use a larger time stepsize in comparison with the traditional methods for numerical solution of semilinear wave equations. This point is significant in the long-time numerical simulation of nonlinear phenomena in a wide variety of practical application areas in Science and Engineering.

The material in this chapter is based on the work by Liu and Wu [56].

References

1. Bátkai, A., Farkas, B., Csomós, P., et al.: Operator semigroups for numerical analysis. 15th Internet Seminar 2011/12 (2011)
2. Hesthaven, J.S., Gottlieb, S., Gottlieb, D.: Spectral methods for time-dependent problems. Cambridge Monographs on Applied and Computational Mathematics. Cambridge University Press, Cambridge (2007)
3. Lakestani, M., Dehghan, M.: Collocation and finite difference-collocation methods for the solution of nonlinear Klein-Gordon equation. Comput. Phys. Commun. **181**, 1392–1401 (2010)
4. Li, S., Vu-Quoc, L.: Finite difference calculus invariant structure of a class of algorithms for the nonlinear Klein-Gordon equation. SIAM J. Numer. Anal. **32**, 1839–1875 (1995)
5. Liu, C., Shi, W., Wu, X.: An efficient high-order explicit scheme for solving Hamiltonian nonlinear wave equations. Appl. Math. Comput. **246**, 696–710 (2014)

6. Shen, J., Tang, T., Wang, L.L.: Spectral Methods: Algorithms, Analysis, Applications. Springer, Berlin (2011)
7. Butcher, J.C.: Numerical Methods for Ordinary Differential Equations, 2nd edn. Wiley, New York (2008)
8. Hairer, E., Lubich, C., Wanner, G.: Geometric Numerical Integration: Structure-preserving Algorithms for Ordinary Differental Equations, 2nd edn. Springer, Berlin (2006)
9. Cohen, D., Jahnke, T., Lorenz, K.C., et al.: Numerical integrators for highly oscillatory Hamiltonian systems: a review. In: Mielke A. Analysis, Modeling and Simulation of Multiscale Problems. Springer, Berlin (2006)
10. García-Archilla, B., Sanz-Serna, J.M., Skeel, R.D.: Long-time-step methods for oscillatory differential equations. SIAM J. Sci. Comput. **20**, 930–963 (1998)
11. Grimm, V.: On error bounds for the Gautschi-type exponential integrator applied to oscillatory second-order differential equations. Numer. Math. **100**, 71–89 (2005)
12. Hochbruck, M., Lubich, C.: A Gautschi-type method for oscillatory second-order differential equations. Numer. Math. **83**, 403–426 (1999)
13. Wu, X., Liu, K., Shi, W.: Structure-Preserving Algorithms for Oscillatory Differential Equations II. Springer, Heidelberg (2015)
14. Wu, X., Wang, B.: Recent Developments in Structure-Preserving Algorithms for Oscillatory Differential Equations. Springer Nature Singapore Pte Ltd., Singapore (2018)
15. Wu, X., You, X., Wang, B.: Structure-Preserving Algorithms for Oscillatory Differential Equations. Springer, Heidelberg (2013)
16. Wu, X., You, X., Xia, J.: Order conditions for ARKN methods solving oscillatory systems. Comput. Phys. Commun. 180: 2250–2257 (2009)
17. Gautschi, W.: Numerical integration of ordinary differential equations based on trigonometric polynomials. Numer. Math. **3**, 381–397 (1961)
18. Hairer, E., Lubich, C.: Long-time energy conservation of numerical methods for oscillatory differential equations. SIAM J. Numer. Anal. **38**, 414–441 (2000)
19. Vanden Berghe, G., de Meyer, H., van Daele, M., et al.: Exponentially fitted Runge–Kutta methods. J. Comput. Appl. Math. **125**, 107–115 (2000)
20. Franco, J.M.: Exponentially fitted explicit Runge–Kutta–Nyström methods. J. Comput. Appl. Math. **167**, 1–19 (2004)
21. Li, Y.W., Wu, X.: Functionally-fitted energy-preserving methods for solving oscillatory nonlinear Hamiltonian systems. SIAM J. Numer. Anal. **54**, 2036–2059 (2016)
22. Franco, J.M.: New methods for oscillatory systems based on ARKN methods. Appl. Numer. Math. **56**, 1040–1053 (2006)
23. Mei, L., Liu, C., Wu, X.: An essential extension of the finite-energy condition for extended Runge–Kutta–Nyström integrators when applied to nonlinear wave equations. Commun. Comput. Phys. **22**, 742–764 (2017)
24. Shi, W., Wu, X., Xia, J.: Explicit Multi-symplectic extended leap-frog methods for Hamiltonian wave equations. J. Comput. Phys. **231**, 7671–7694 (2012)
25. Wang, B., Wu, X.: Long-time momentum and actions behaviour of energy-preserving methods for semilinear wave equations via spatial spectral semi-discretizations. Adv. Comput. Math. **45**, 2921–2952 (2019)
26. Wu, X., Wang, B., Shi, W.: Efficient energy-preserving integrators for oscillatory Hamiltonian systems. J. Comput. Phys. **235**, 587–605 (2013)
27. Wu, X., You, X., Shi, W., et al.: ERKN integrators for systems of oscillatory second-order differential equations. Comput. Phys. Commun. **181**, 1873–1887 (2010)
28. Liu, C., Iserles, A., Wu, X.: Symmetric and arbitrarily high-order Birkhoff-Hermite time integrators and their long-time behaviour for solving nonlinear Klein-Gordon equations. J. Comput. Phys. **356**, 1–30 (2018)
29. Liu, C., Wu, X.: Arbitrarily high-order time-stepping schemes based on the operator spectrum theory for high-dimensional nonlinear Klein-Gordon equations. J. Comput. Phys. **340**, 243–275 (2017)

30. Wang, B., Iserles, A., Wu, X.: Arbitrary-order trigonometric Fourier collocation methods for multi-frequency oscillatory systems. Found. Comput. Math. **16**, 151–181 (2016)
31. Wang, B., Wu, X., Meng, F.: Trigonometric collocation methods based on Lagrange basis polynomials for multi-frequency oscillatory second-order differential equations. J. Comput. Appl. Math. **313**, 185–201 (2017)
32. Wu, X., Wang, B., Mei, L.: Oscillation-preserving algorithms for efficiently solving highly oscillatory second-order ODEs. Numer. Algor. **86**, 693–727 (2021)
33. van der Houwen, P.J., Sommeijer, B.P.: Explicit Runge–Kutta(–Nyström) methods with reduced phase errors for computing oscillating solutions. SIAM J. Numer. Anal. **24**, 595–617 (1987)
34. Dehghan, M., Mohebbi, A., Asgari, Z.: Fourth-order compact solution of the nonlinear Klein–Gordon equation. Numer. Algor. **52**, 523–540 (2009)
35. Dehghan, M., Shokri, A.: Numerical solution of the nonlinear Klein-Gordon equation using radial basis functions. J. Comput. Appl. Math. **230**, 400–410 (2009)
36. Dehghan, M., Ghesmati, A.: Application of the dual reciprocity boundary integral equation technique to solve the nonlinear Klein–Gordon equation. Comput. Phys. Commun. **181**, 1410–1418 (2010)
37. Shakeri, F., Dehghan, M.: Numerical solution of the Klein–Gordon equation via He's variational iteration method. Nonlinear Dynam. **51**, 89–97 (2008)
38. Cano, B.: Conservation of invariants by symmetric multistep cosine methods for second-order partial differential equations. BIT Numer. Math. **53**, 29–56 (2013)
39. Cohen, D., Hairer, E., Lubich, C.: Conservation of energy, momentum and actions in numerical discretizations of non-linear wave equations. Numer. Math. **110**, 113–143 (2008)
40. Dong, X.: Stability and convergence of trigonometric integrator pseudo spectral discretization for N-coupled nonlinear Klein-Gordon equations. Appl. Math. Comput. **232**, 752–765 (2014)
41. Gauckler, L.: Error analysis of trigonometric integrators for semilinear wave equations. SIAM J. Numer. Anal. **53**, 1082–1106 (2015)
42. Hochbruck, M., Pažur, T.: Error analysis of implicit Euler methods for quasilinear hyperbolic evolution equations. Numer. Math. **135**, 547–569 (2017)
43. Wang, B., Wu, X.: The formulation and analysis of energy-preserving schemes for solving high-dimensional nonlinear Klein-Gordon equations. IMA J. Numer. Anal. **39**(4), 2016–2044 (2019)
44. Wang, B., Wu, X.: Globel error bounds of one-stage extended RKN integrators for semilinear wave equations. Numer. Algor. **81**, 1203–1218 (2019)
45. Liu, C., Wu, X.: The boundness of the operator-valued functions for multidimensional nonlinear wave equations with applications. Appl. Math. Lett. **74**, 60–67 (2017)
46. Liu, C., Wu, X.: An energy-preserving and symmetric scheme for nonlinear Hamiltonian wave equations. J. Math. Anal. Appl. **440**, 167–182 (2016)
47. Wu, X., Liu, C.: An integral formula adapted to different boundary conditions for arbitrarily high-dimensional nonlinear Klein-Gordon equations with its applications. J. Math. Phys. **57**(2), 3239–3249 (2016)
48. Wu, X., Liu, C., Mei, L.: A new framework for solving partial differential equations using semi-analytical explicit RK(N)-type integrators. J. Comput. Appl. Math. **301**, 74–90 (2016)
49. Wu, X., Mei, L., Liu, C.: An analytical expression of solutions to nonlinear wave equations in higher dimensions with Robin boundary conditions. J. Math. Anal. Appl. **426**, 1164–1173 (2015)
50. Gottlieb, D., Orszag, S.: Numerical Analysis of Spectral Methods: Theory and Applications. Society for Industrial and Applied Mathematics, Philadelphia (1993)
51. Tang, W.S., Ya, Y.J., Zhang, J.J.: High order symplectic integrators based on continuous-stage Runge–Kutta–Nyström methods. Appl. Math. Comput. **361**, 670–679 (2019)
52. Mei, L., Wu, X.: The construction of arbitrary order ERKN methods based on group theory for solving oscillatory Hamiltonian systems with applications. J. Comput. Phys. **323**, 171–190 (2016)

53. Wang, B., Liu, K., Wu, X.: A Filon-type asymptotic approach to solving highly oscillatory second-order initial value problems. J. Comput. Phys. **243**, 210–223 (2013)
54. Bao, W.Z., Dong, X.C.: Analysis and comparison of numerical methods for the Klein-Gordon equation in the nonrelativistic limit regime. Numer. Math. **120**, 189–229 (2012)
55. Wang, Y., Zhao, X.F.: Symmetric high order Gautschi-type exponential wave integrators pseudospectral method for the nonlinear Klein-Gordon equation in the nonrelativistic limit regime. Int. J. Numer. Anal. Mod. **15**(3), 405–427 (2018)
56. Liu, C., Wu, X.: Nonlinear stability and convergence of ERKN integrators for solving nonlinear multi-frequency highly oscillatory second-order ODEs with applications to semi-linear wave equations. Appl. Numer. Math. **153**, 352–380 (2020)